PEOPLE'S DEMOCRATIC REPUBLIC OF ALGERIA

Ministry of Higher Education and Scientific Research

University of 20 August 1955 – SKIKDA



Faculty of Science, Department of Chemistry

Master's Thesis

Field: Chemistry

Specialty: Organic Chemistry

Presented by:

GABLI AYA

Synthesis and Molecular Modelling of Stabilising Additives for Bitumen Storage at Reduced Temperature.

Date of Defense: 07/07/2026

Board of Examiners

President	**:** Dr. MEGUELLATI Amel	University of Skikda	(MCB)
Supervisor	**:** Dr. CHEKKAL Faiza	University of Skikda	(MCA)
Co-Supervisor	**:** Dr. BOUGHAZI Hind	University of Skikda	(MCB)
Examiner	**:** Dr. YAHIAWassila	University of Skikda	(MCA)

Acknowledgements

First and foremost, I would like to express my deepest gratitude to Allah, the Most Merciful, for granting me the strength, determination, perseverance, and patience to complete this work and pursue my studies successfully throughout these years.

I would like to express my sincere appreciation to Dr. Faiza Chekkal, my supervisor at the University of Skikda, for accepting this work and for her valuable guidance, insightful advice, openness, and constant availability throughout the project's development.

I would also like to extend my sincere thanks to all the staff of the RA1K Refinery Laboratory in Skikda for their support and cooperation.

Finally, I would like to thank my Co-Supervisor, Dr. BOUGHAZI Hind, and the Course Director of the Organic Chemistry Department, Dr. Nedjma Melais, and all the staff members of the Department of Chemistry and the Faculty of Materials Science, for their contribution to my academic training and education.

"Thank you all."

Dedication

With the utmost affection and gratitude, I dedicate this humble work to those whose love and steadfast devotion have been the greatest blessings of my life.

To my beloved Mother **ZAITE HABIBA**, the one and only, who chose us over her own life, and whose affection, wisdom, and sacrifices have been my greatest blessing. Whatever honour this work may possess is, in great measure, owing to you.

To my dear Father, my guardian angel **GABLI SALIM**, though your absence graces this day with a melancholy, your enduring influence remains ever present in my heart. It is my sincerest hope that this humble achievement may serve to elevate your honour and bring serenity to your noble soul.

To my dear brother **ABDE ARAHMENE** and beloved sisters **AMINA** and **IMEN**, whose unwavering support, affection, and companionship have been a constant source of strength and comfort.

To my cherished grandparents, esteemed family, and treasured friends, my deepest gratitude for your love and encouragement.

I want to express my heartfelt gratitude for your kindness, good wishes, and encouragement. Your support has enriched my life beyond measure.

May the Almighty bestow upon you health, happiness, prosperity, and every blessing.

With enduring affection and the highest esteem, Yours truly,

Aya Gabli

Abstract

The grade 70/100 bitumen produced by the RA1K refinery of Skikda (**SONATRACH**) is the reference road binder in Algeria. During high-temperature storage (150–200 °C), it undergoes progressive **oxidative ageing**, **colloidal instability** driven by **asphaltene** aggregation, and **viscosity increase**. This work combines organic synthesis, UV-visible characterisation, and **DFT molecular modelling** (ωB97X-D/6-311++G(d,p)) to evaluate three complementary **stabilising additives** 2,6-di-tert-butylphenol (PHEN), N-phenylbenzamide (BENZ), benzyl benzoate (PLAS) — plus n-octacosane (CIRE). **Interaction energies** across 16 additive–SARA complexes show BENZ has the highest affinity for the full bituminous system (ΔEint = −66.94 kcal/mol via 12 π–π contacts), PHEN binds the asphaltene model via O–H···N bonds (−13.80 kcal/mol), and CIRE inserts into the saturated fraction (−15.49 kcal/mol). The synergistic combination is projected to lower mixing temperatures by 20–40 °C, enabling **WMA** technology in the Algerian industrial context.

Résumé

Le **bitume de grade 70/100** produit par la raffinerie RA1K de Skikda (**SONATRACH**) constitue le liant routier de référence en Algérie. Lors de son stockage à haute température (150–200
°C), il est soumis au **vieillissement oxydatif** radicalaire, à **l'instabilité colloïdale** liée à l'agrégation des **asphaltènes** et à une augmentation de viscosité compromettant sa mise en œuvre industrielle. Ce mémoire développe et évalue, par une approche combinant synthèse organique et **modélisation moléculaire DFT** (ωB97X-D/6-311++G(d,p)), **trois additifs stabilisants** complémentaires : le 2,6-di-tert-butylphénol (PHEN, **antioxydant primaire**), le N-phénylbenzamide (BENZ, stabilisateur colloïdal) et le benzoate de benzyle (PLAS, **modificateur de viscosité**), auxquels s'ajoute le n-octacosane (CIRE) comme **réducteur de température de transition**. Les calculs d'énergie d'**interaction** sur les 16 complexes additif–SARA montrent que BENZ présente l'affinité la plus élevée pour le système bitumineux complet (ΔEint = −66,94 kcal/mol via 12 interactions π–π), que PHEN interagit préférentiellement avec la fraction asphaltène par liaisons O–H···N (−13,80 kcal/mol), et que CIRE s'insère sélectivement dans la fraction saturée (−15,49 kcal/mol). La synergie des trois additifs est susceptible d'abaisser la température de mise en œuvre de 20 à 40 °C, ouvrant la voie aux **enrobés tièdes (WMA)** dans le contexte industriel algérien.

الملخص

يُعدّ **البيتومين من الدرجة 70/100** المنتج بمصفاة RA1Kبسكيكدة التابعة لشركة **سوناطراك** المادة الرابطة المرجعية المستخدمة في رصف الطرق في الجزائر. وأثناء تخزينه في درجات حرارة مرتفعة تتراوح بين 150و022 °م، يتعرض لظاهرة **التقادم التأكسدي الجذري، وعدم الاستقرار الغروي** الناتج عن تكتل **الأسفلتينات**، بالإضافة إلى **زيادة في اللزوجة**، مما يؤثر سلبًا على سهولة معالجته وتطبيقه في العمليات الصناعية.

يهدف هذا العمل إلى تطوير وتقييم، من خلال منهج يجمع بين **التخليق العضوي والنمذجة الجزيئية** باستخدام نظرية دالة الكثافة (**DFT**) عند مستوى ωB97X-D/6-311++G(d,p)، ثلاثة إضافات تثبيتية متكاملة، وهي-2,6 :ثنائي ثالثي بيوتيل فينول (PHEN) **كمضاد أكسدة** أولي، و-Nفينيل بنزاميد (BENZ) **كمثبت غروي**، وبنزوات البنزيل (PLAS) **كمعدل للزوجة**، بالإضافة إلى الن-أوكتاكوسان (CIRE) **كمخفض لدرجة حرارة** التشغيل.

أظهرت حسابات طاقة التفاعل بين الإضافات ومكونات البيتومين الأربع (SARA) على مستوى 16معقدًا أن مركب BENZيمتلك أعلى ألفة تجاه النظام البيتومين الكامل، حيث بلغت طاقة التفاعل(ΔEint = −66.94 kcal/mol) ، وذلك بفضل تكوين 12تفاعلًا من نوع .π–π كما تبين أن PHENيتفاعل بصورة تفضيلية مع جزء الأسفلتينات من خلال روابط هيدروجينية من النوع O–H•••Nبطاقة تفاعل قدرها 13.80 kcal/mol−، في حين يندمج CIREبشكل انتقائي داخل الجزء المشبع بطاقة تفاعل بلغت .15.49 kcal/mol−

وتشير النتائج إلى أن التأثير التآزري لهذه الإضافات الثلاث من شأنه أن يُخفض درجة حرارة تشغيل البيتومين بمقدار يتراوح بين 20و02 °م، مما يفتح آفاقًا واعدة لاعتماد **تقنية الخلطات الإسفلتية الدافئة (Warm Mix Asphalt, WMA)** في القطاع الصناعي الجزائري.

Table of Contents

	List abbreviated	**III**
	List of Table	**IV**
	List of Figures	**V**
	Introduction	1
	Chapter I: Bitumen Properties, Storage, and Associated Problems	
	Introduction	4
I.1.	Definition and origin of bitumen	4
I.1.1.	Definition	4
I.1.2.	Natural and Industrial Origins	5
I.2.	Chemical composition: the SARA model	7
I.2.1.	Colloidal Structure: Sol, Gel, and Sol-Gel	10
I.3.	Physicochemical properties	11
I.3.1.	Viscosity and temperature dependence	11
I.3.2.	Softening point and thermal sensitivity	12
I.3.3.	Thermal stability	12
I.3.4.	Other essential properties	13
I.4.	Storage problems	14
I.4.1.	Oxidative ageing	14
I.4.2.	Phase separation and colloidal instability	15
I.4.3.	Thermal and exudation problems	15
I.4.4.	Corrosion by naphthenic acidity	16
I.4.5.	Health, safety, and industrial hazards	16
I.5.	Chemical solution: additives to improve stability and reduce processing temperature	17
	Conclusion	17
	References	18

Table of Contents

Chapter II: Bitumen Stabilising Additives

	Introduction	19
II.1.	General role of additives in bitumen	19
II.1.1.	Antioxidants	20
II.1.2.	Thermal stabilisers	20
II.1.3.	Dispersing agents and viscosity modifiers	20
II.2.	Mechanisms of action	20
II.2.1	Free radical inhibition	20
II.2.2.	Stabilisation of asphaltenes	20
II.2.3	Improved fluidity and reduced implementation temperature	21
II.3.	Classification and examples of additives used in industry	21
II.4.	Criteria for selecting additives	22
II.4.1.	Functional efficiency	22
II.4.2.	Thermal stability	22
II.4.3.	Compatibility with bitumen	22
II.4.4.	Cost and availability in the Algerian context	23
II.5.	Choice and justification of the additives used in this work	23
II.5.1.	Additive 1: 2,6-di-tert-butylphenol Primary antioxidant	23
II.5.2.	Additive 2: N-phenyl-benzamide (benzanilide) Colloidal stabilizer	24
II.5.3	Additive 3: Benzyl benzoate Viscosity modifier/plasticiser	24
II.5.4	Expected synergy of the three additives	25
	Conclusion	25
	References	26

Chapter III: Foundations of Molecular Modelling

	Introduction	28
III..1.	The value of molecular modelling for bituminous systems	28
III.2.	Molecular representation of bitumen	29
III.2.1.	SARA Approach	29
III.2.2.	Representation of asphaltenes	30
III.2.3.	Model Molecules	30
III.3.	Principles of molecular modelling methods	31

III.3.1.	Geometric Optimisation	31
III.3.2	Semi-empirical methods	32
III.3.3.	Density Functional Theory (DFT)	32
III.3.4.	Basic Sets	33
III.3.5.	Functionalities of the DFT	33
III.3.6.	Molecular Dynamics (MD)	34
III.4.	Theoretical quantities used in molecular modelling	35
III.4.1.	Interaction Energy	35
III.4.2.	HOMO and LUMO frontier orbitals	35
III.4.3.	Electron density	36
III.4.4.	Weak intermolecular interactions	36
III.5.	Recent applications and perspectives	37
	Conclusion	38
	References	39

Chapter IV: Methodological Section

IV.I	EXPERIMENTAL METHODOLOGY	41
IV.I.1	Additive synthesis strategy	41
IV.I.1.1	Choice of precursors and justification	41
IV.I.1.2	Selection of reactions	42
IV.I.2	Experimental synthesis protocols	42
IV.I.2.1	Synthesis of 2,6-di-tert-butylphenol (PHEN)	42
IV.I.2.2	Synthesis of N-phenyl-benzamide (BENZ)	45
IV.I.2.3	Synthesis of benzyl benzoate (PLAS)	47
IV.I.2.4	Commercial additive: N-Octacosane (CIRE)	50
IV.I.3.	Experimental characterisation of additives	50
IV.I.3.1	Analytical techniques used	50
IV.I.32	Characterisation Data	50
IV.II.	MOLECULAR MODELING METHODOLOGY	51
IV.II.1.	Selection of model molecules	51
IV.II.1.1	Additive studied	51
IV.II.1.2	Representative molecular models of SARA fractions	51
IV.II.2.	Computational Environment and Software	52

IV.II.3. DFT Calculation Parameters 52
IV.II.3.1 Choice of the functional 52
IV.II.3.2 Calculation parameters 53
IV.II.3.3 Solvation Model 53
IV.II.4. Calculation Protocols 53
IV.II.4.1 Geometric optimisation of monomers 53
IV.II.4.2 Post-calculation analyses 54
References 55

Chapter V: Results and Discussion

V.I. Experimenta results 56
V.I.1. Synthesis and characterisation results of additives 56
V.I.1.1. Yields and appearance of the production obtained 56
V.I.1.2. Characterisation by UV-visible spectroscopy 56
V.I.2. Structural confirmation by comparison with the literature 57
V.II.1. Molecular modelling results 58
V.II.1.1. Geometric optimisation of additives and bitumen models 58
V.II.1.2. Electronic properties of additives HOMO 61
V.II.1.3. Additive interaction energies -SARA 64
Conclusion 69
ACKNOWLEDGMENTS ..... **I**
Dedication ..... **II**
Abstract ..... **II**

List of abbreviations

Abbreviation	Full meaning
AcOEt	Ethyl acetate TLC eluent (hexane/ AcOEt mixture)
ACID	Benzoic acid ($C_7H_6O_2$) Molecular model of resins
ATG / TGA	Thermogravimetric Analysis Analysis
BBR	Bending Beam Rheometer on beams under low-temperature bending conditions (EN 14771)
BENZ	N- phenyl-benzamide / benzanilide (A_2) Colloidal stabiliser
B3LYP-D3	Grimme dispersion correction (3rd generation)
BIOVIA DS	BIOVIA Discovery Studio Visualizer 2021 Analysis of non-covalent interactions
CI	Carbonyl Index Carbonyl index measured by FTIR (~1700 cm^{-1})
CII	Colloidal Instability Index Colloidal instability index = (Sat + Asph) / (Arom + Res)
COMPASS III	Condensed-phase Optimised Molecular Potentials for Atomistic Simulation Studies Force field (Material Studio)
CORO	Coronene ($C_{24}H_{12}$) Molecular Model of Aromatics
^{13}C NMR	Carbon-13 NMR
CCM / TLC	Thin Layer Chromatography
DCM	Dichloromethane Benzyl Synthesis Solvent
ΔEgap	HOMO-LUMO energy difference Electron gap (eV)
ΔEint	Interaction energy of a molecular complex (kcal/mol)
DFT	Density Functional Theory Density Functional Theory
DSR	Dynamic Shear Rheometer Dynamic shear rheometer (EN 14770)
EDA	Energy Decomposition Analysis: Decomposition of interaction energy
ESP	Electrostatic Surface Potential Electrostatic Surface Potential Map
EVA	Ethylene-Vinyl Acetate Bitumen Modifying Polymer
FTIR	Fourier Transform Infrared Spectroscopy Fourier Transform Infrared Spectroscopy
G09	Gaussian 09 DFT calculation software (Frisch et al.)
HAT	Hydrogen Atom Transfer Transfer of hydrogen atoms (antioxidant mechanism)
^{1}H NMR	proton NMR (300 MHz, $CDCl_3$ solvent)
HOMO	Highest Occupied Molecular Orbital Highest occupied molecular orbital
IGMH	Independent Gradient Model based on Hirshfeld partition (Lu & Chen, 2021)
IGM	Independent Gradient Model
ILO	Oxidation Induction Time Oxidation induction time (ASTM E1641)
LUMO	Lowest Unoccupied Molecular Orbital Lowest unoccupied molecular orbital
M06-2X	Minnesota meta-functional adapted to non-covalent interactions

List of abbreviations

MD	Molecular Dynamics
Multiwfn	Wave function analysis software (version 3.8, Lu & Chen, 2012)
η	Overall chemical hardness $\eta = ½ (E_{LUMO} - E_{HOMO})$ in eV
NAFTAL	National Company for the Marketing and Distribution of Petroleum Products (Algeria)
NBO	Natural Bond Orbital Natural Bond Orbitals
NCI	Non-Covalent Interactions A method for visualising non-covalent interactions (Johnson et al., 2010)
NMR / NMR	Nuclear Magnetic Resonance Magnetic Resonance
σ	Overall chemical softness $\sigma = 1/2\eta$ in eV^{-1}
PAH	Polycyclic Aromatic Hydrocarbon Polycyclic Aromatic Hydrocarbon
PAV	Pressure Ageing Vessel Long-term ageing under pressure (EN 14769, 100 °C, 2.1 MPa, 20 h)
PCM	Polarizable Continuum Model Polarizable continuum model
PHEN	2,6-Di-tert-butylphenol (A_1) Primary antioxidant
PI	Penetration Index Penetration index (thermal susceptibility)
PORP	Porphyrin Ni (II) ($C_{20}H_{14}N_4Ni$) Molecular model of Asphaltenes
QTAIM	Quantum Theory of Atoms in Molecules Quantum Theory of Atoms in Molecules (Bader)
RES	National Refining Company (Algeria)
RTFOT	Rolling Thin Film Oven Test Short-term ageing (EN 12607-1, 163 °C, 85 min)
SARA	Saturates Aromatics Resins Asphaltenes Fractionation of bitumen (ASTM D4124)
SBS	Styrene-Butadiene-Styrene Bitumen-modifying triblock copolymer
SDA	Solvent Deaphalting Solvent-based deasphalting
Student Union	Bond Dissociation Energy O–H Bond Dissociation Energy
SQUA	Squalene ($C_{30}H_{62}$) Molecular Model of Saturates
TAN	Total Acid Number Total naphthenic acidity index (ASTM D664, mg KOH/g)
μ	Electronic chemical potential $\mu = ½ (E_{HOMO} + E_{LUMO})$ in eV
UV-vis	UV-visible absorption spectroscopy (200–400 nm)

List of abbreviations

VMD	Visual Molecular Dynamics 3D molecular visualization software (v1.9.4)
WAX	N-Octacosane $C_{28}H_{58}$ (A_4) Transition temperature reducing agent
WMA	Warm Mix Asphalt Warm mix asphalt (reduced temperature of 20–50 °C)
ωB97X-D	Hybrid functional span separation with D2 dispersion correction (Chai & Head-Gordon, 2008)
ω	electrophilicity index $\omega = \mu^2/2\eta$ in eV
χ	Overall electronegativity $\chi = -\mu$ in eV

List of Tables

ble I.1	Comparative properties of the four SARA fractions of bitumen (compiled from)	8
Table I.2.	Physicochemical specifications for road bitumens 35/50 and 50/70 according to EN 12591	13
Table II.1	Presents a cross-classification of the main industrial additives according to their function and area of application	21
Table II.2.	Summarises the complementarity of the three additives with respect to the degradation mechanisms of 70/100 bitumen	25
Table.III.1.	Recommended DFT functionals for the study of bituminous systems...	32
Table IV.I.1	Precursors and target functional groups	41
Table IV.I.2	Selection of reactions and justifications	42
Table IV.I.3	Reagents for the synthesis of PHEN	43
Table IV.I.4	Reagents for the synthesis of BENZ	45
Table IV.I.5	Reagents for PLAS synthesis	48
Table IV.I.6	Spectroscopic and Physicochemical Characterisation of the Synthesised 4Additives (PHEN, BENZ, PLAS, and CIRE)	50
TableIV.II.1	Modelled additives and expected mechanisms of action	51
Table IV.II.2	SARA molecular models: rationale and limitations	51
Table IV.II.3	Software used	52
Table IV.II.4	DFT Parameters	53
Table IV.II.5	Post-calculation analysis methods	54
Table V.I.1	Physical characterisation and yields of additives synthesised in thelaboratory	56
Table V.I.2	UV-visible data for the four additives (EtOH, 10^{-4} mol·L^{-1})	57
Table V.I.3	Reference spectroscopic data (literature) for the four additives	58
Table V.II.1	Main geometric parameters of the four additives optimised at the wB97X-D/6-311++G (d, p) level	60
Table V.II.2	Energy parameters and overall reactivity descriptors of the additives studied	61
Table V.II.3	Overall reactivity descriptors of SARA model molecules	62
Table V.II.4	Interaction energies ΔEint (kcal/mol) of the 16 additive-SARA complexes Calculated by Material Studio	65
Table V.II.5	Interaction energies ΔEint (kcal/mol) of additives with the complete SARA system and molecular interpretation	66

List of Tables

Table V.II.6 Non-covalent interactions of additive-SARA complexes analysed using Discovery Studio. Types, number and distances of π-π stacking interactions, and corresponding global interaction energies..... 67

List of Figures and schema

Figure I.1	Solid Bitumen	5
Figure I.2	Penetrometer	5
Figure I.3	Example of a resin chemical structure: 3-methyl-dibenzothiophene ($C_{13}H_{10}S$)	9
Figure I.4	Colloidal models of bitumen: Sol ("island") and Gel ("continental") structures, with Sol-Gel as the intermediate case for road bitumens	10
Figure II.1	chemical structure of 2, 6-di-tert-butylphenol	23
Figure II.2	chemical structure of N-phenyl-benzamide	24
Figure II.3	chemical structure of benzyl benzoate	24
Figure III.1	Representation Schematic of the SARA fractions of bitumen and corresponding model molecules	31
Figure III.2	Schematic representation of weak intermolecular interactions in a bituminous system	37
Figure IV.I.1	Reaction scheme for the synthesis of 2,6-di-tert-butylphenol (PHEN)	42
Figure IV.I.2	Experimental setup for the synthesis of PHEN	44
Figure IV.I.3	PHEN product obtained	44
Figure IV.I.4	Reaction scheme for the synthesis of N-phenyl-benzamide (BENZ) by acylation of aniline	45
Figure IV.I.5	Photograph of the experimental setup for the synthesis of BENZ	46
Figure IV.I.6	Product BENZ (N-phenyl-benzamide) recrystallised in ethanol	47
Figure IV.I.7	Reaction scheme for the synthesis of benzyl benzoate (PLAS) by Fischer Esterification	47
Figure IV.I.8	PLAS synthesis setup	49
Figure IV.I.9	PLAS (benzyl benzoate) product after distillation	49
Figure V.II.1	Optimised structures of additives (PHEN, BENZ, PLAS, CIRE) obtained at the theoretical level wB97X-D/6-311++G (d,p)	59
Figure V.II.2	Optimised structures of the SARA models (ACID, CORO, PORP, SQUA) obtained at the theory level wB97X-D/6-311++G (d,p)	60
Figure V.II.3	Representation of the HOMO and LUMO frontier orbitals of the additives PHEN (A_1), BENZ (A_2), PLAS (A_3), and CIRE (A_4) calculated at the theoretical ωB97X-D/6-311++G (d, p) level	63

List of Figures and schema

Figure V.II.4	ESP maps of the four additives studied at the ωB97X-D/6-311++G level (d, p) (iso = 0.004 a.u.) (red: nucleophilic region; blue: electrophilic region.....	64
Figure V.II.5	Interaction energies ΔEint (kcal/mol) for 16 additive-SARA complexes.....	65
Figure V.II.6	Interaction energies ΔEint (kcal/mol) of the four additives with the complete SARA system (SQUA + CORO + ACID PORP)	66
Figure V.II.7	Representation of non-covalent interactions of additives-SARA complexes (PHEN/A1, BENZ/A2, PLAS-A3, CIRE-A4) visualized under discovery studio client…….	68
Schema I.1	Schematic of bitumen production by petroleum refining (atmospheric distillation → vacuum distillation →bitumen)	7
Schema I.2	Schematic of SARA fractionation (n-heptane precipitation of asphaltenes, then Iatroscan chromatography separating saturates, aromatics, and resins from the maltene fraction)	9

Introduction

Introduction

Bitumen is one of the oldest materials used by humankind, with documented traces dating back to 3800 BCE. Today, it is the essential hydrocarbon binder for the construction and maintenance of road pavements, representing approximately 90% of global consumption. In Algeria, grade 70/100 bitumen produced by the RA1K refinery in Skikda, operated by SONATRACH, is the national reference source. Obtained by atmospheric and then vacuum distillation of heavy crude oil, this binder is used in all road projects undertaken by national companies in the sector, such as NAFTAL and ENR. Its economic and technical importance is therefore considerable for the development of Algerian infrastructure. However, the production and industrial application of bitumen require prolonged storage at high temperatures, maintained between 150°C and 200°C, to preserve the fluidity necessary for pumping and mixing with aggregates. These severe thermal conditions subject the bitumen to several cumulative and irreversible degradation mechanisms. The first is radical oxidative ageing: dissolved oxygen reacts with the aromatic and naphthenic fractions according to a chain radical kinetics, leading to the formation of polar oxygenated groups—carbonyls and sulfoxides—which progressively stiffen the binder, increase its softening point, and decrease its penetrability. The second phenomenon is colloidal instability: bitumen is a colloidal system whose stability depends on the balance between its four constituent fractions, described by the SARA model (Saturates, Aromatics, Resins, Asphaltenes). The oxidation of the resins, which act as peptizers for the asphaltene micelles, disrupts this balance and leads to the sedimentation of asphaltene aggregates at the bottom of the tanks, irreparably altering the quality of the delivered binder. In addition to these two mechanisms, there is the progressive increase in viscosity, resulting from the conversion of the lighter fractions into heavy polar products, which makes pumping and applying the bitumen increasingly difficult and energy-intensive. Faced with these challenges, the formulation of targeted chemical additives is emerging as a leading technological solution. When judiciously selected and combined, antioxidants, colloidal stabilisers, and viscosity modifiers can simultaneously counteract these degradation mechanisms, lower storage and application temperatures by 20 to 40 °C, and pave the way for warm mix asphalt (WMA) technologies, the large-scale adoption of which would represent a significant economic and environmental gain for the Algerian road construction sector.

Understanding the interaction mechanisms between these additives and the different fractions of bitumen at the molecular level is therefore a scientific and industrial challenge of paramount

importance. It is within this specific context, rooted in the industrial reality of the RA1K refinery in Skikda, that the present work is situated. Three additives with complementary chemical functions were selected and then synthesised in the laboratory from precursors available in the Algerian industrial context. 2,6-Di-tert-butylphenol (PHEN) was chosen as the primary antioxidant: A phenol sterically hindered by two tert-butyl groups in ortho positions, it acts via the hydrogen atom transfer (HAT) mechanism, interrupting the free radical oxidation chain.

N-Phenylbenzamide (BENZ) is used as a colloidal stabiliser: its polar amide group forms hydrogen bonds with the heteroatoms of asphaltenes, while its two phenyl rings establish π–π interactions with the polyaromatic sheets, promoting the peptization of the micelles and delaying their sedimentation. Benzyl benzoate (PLAS) is used as a plasticiser and viscosity modifier: by increasing the free volume of the bituminous matrix, it reduces intermolecular interactions and lowers the apparent viscosity of the binder. A fourth compound, n-octacosane (CIRE, $C_{28}H_{58}$), is included in the study due to its melting point of 61–63 °C, perfectly suited to the summer service temperatures of Algerian pavements, allowing for reversible crystallisation that strengthens the bitumen matrix in situ. The approach adopted is decidedly two-dimensional. Experimentally, the three additives were synthesised using appropriate reaction routes and characterised by UV-visible spectroscopy and thin-layer chromatography. Computationally, Density Functional Theory (DFT) was applied at the theoretical level ωB97X-D /6-311++G(d,p) was implemented to analyze the electronic properties of the four additives and quantify their interaction energies with molecular models representative of the four SARA fractions: squalane for the Saturates, coronene for the Aromatics, benzoic acid for the Resins, and Ni(II) porphyrin for the Asphaltenes. This hybrid span-separation functional, equipped with a D2 dispersion correction, is particularly well-suited to describing the dominant non-covalent interactions in bituminous systems, including π–π interactions, hydrogen bonds, and van der Waals forces.

This thesis is organised into five progressive and logically linked chapters. The first chapter presents the physicochemical properties of bitumen, its storage conditions at the RA1K refinery in Skikda, and the degradation phenomena to which it is exposed, as well as the available chemical solutions.

The second chapter is devoted to stabilising additives, covering their mechanisms of action, industrial classification, selection criteria, and the rationale behind the compounds chosen in the Algerian context.

The third chapter presents the theoretical foundations of molecular modelling applied to bituminous systems, from the SARA representation and the Yen-Mullins model for asphaltenes to DFT methods and tools for analysing non-covalent interactions.

The fourth chapter describes the complete methodology adopted, both experimental and computational. Finally, the fifth chapter presents and discusses all the results obtained, highlighting the complementarity and synergy of the additives developed with respect to the mechanisms of bitumen degradation from the R1K refinery in Skikda.

Chapter I:

Bitumen Properties, Storage, And Associated Problems

Introduction

Bitumen is one of the oldest materials used by humankind, with documented use dating back to 3800 BC for waterproofing purposes. Today, it plays a vital role in road construction, representing approximately 90% of its global consumption.**[1]**

Its importance stems from a unique combination of physicochemical properties, adhesiveness, waterproofing, thermoplasticity, and viscoelasticity that make it irreplaceable in pavement engineering.

However, biumen is a chemically complex and thermosensitive material. Its performance depends critically on its colloidal microstructure, which is governed by the balance between its molecular fractions. This balance is fragile: during storage at temperatures of 150–200°C, oxidation, phase separation, and thermal degradation progressively alter the binder's properties.**[2]**

This chapter presents, in a logically connected progression, the definition and origin of bitumen, its chemical composition according to the SARA model, the colloidal structure that results from it, the physicochemical properties derived from that structure, in particular viscosity, softening point, and thermal stability, followed by the storage problems these properties generate, and finally the chemical solutions available through additives.

I. 1: Definition and Origin of Bitumen

I. 1.1: Definition

Bitumen is a complex mixture of high molecular weight hydrocarbons, practically non-volatile, with strongly adhesive and hydrophobic character. It is found either naturally in the environment or is produced industrially by the distillation of certain crude oils.

At room temperature, it behaves as a viscoelastic solid; when heated above approximately 120°C, it becomes a viscous and workable liquid.**[3]**



Figure I.1: solid bitumen.

Bitumen grades are defined by their **penetration at 25°C**, measured using a penetrometer, in tenths of a millimetre (0.1 mm) under a standard needle load of 100 g for 5 seconds (EN 1426). The grade designation indicates the penetration range: a **35/50** bitumen has a penetration between 35 and 50 × 0.1 mm; it is hard and stiff, suited to hot climates. A **50/70** bitumen (50–70 × 0.1 mm) is softer and more workable, suited to temperate regions.

The higher the penetration, the softer the bitumen**.[4]**



Figure I.2: Penetrometer.

I. 1.2: Natural and Industrial Origins

Bitumen occurs naturally in asphalt rock deposits (e.g., Trinidad and Tobago, Val-de-Travers in Switzerland) and in oil sands (Alberta, Canada).

However, the vast majority of industrial bitumen is obtained from the **vacuum distillation of heavy crude oils**. The production process involves two successive stages: **[3]**

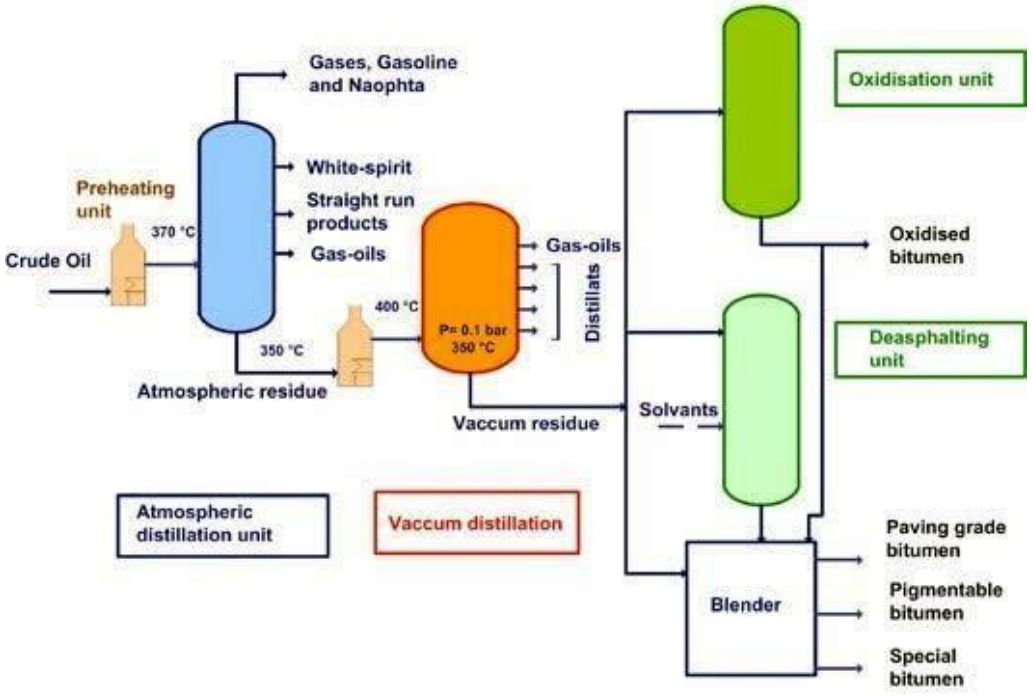
- **Atmospheric distillation:** crude oil is heated to 350–380°C at the base of a distillation column. Light fractions (LPG, gasoline, kerosene, diesel) are separated progressively from top to bottom according to their boiling points. The heavy residue remaining at the bottom is called the atmospheric residue.

- **Vacuum distillation:** the atmospheric residue is further distilled under reduced pressure (4–13 kPa), allowing separation of lubricating oils without thermal cracking. The residue remaining after this stage is direct-distillation bitumen.

Two complementary processes exist for producing bitumens with specific properties:

- **Air blowing (oxidation):** hot air at 230–270°C is blown through the vacuum residue. Controlled oxidation increases the softening point and reduces temperature sensitivity. The resulting 'blown bitumen' is stiffer and more elastic, used in industrial applications (roofing, waterproofing) rather than road paving.

- **Solvent deasphalting (SDA):** a light solvent (propane or butane) is passed upward through the vacuum residue. The difference in solubility between the heavy asphaltenic fraction and the lighter components causes selective precipitation of asphaltenes, yielding a bitumen of low penetrability with a high lubricating fraction



Schema I.1: Schematic of bitumen production by petroleum refining (atmospheric distillation → vacuum distillation → bitumen)**.[12]**

I. 2: Chemical Composition: the SARA Model

Bitumen is not a pure compound but a polydisperse colloidal system. Its chemical characterisation relies on the **SARA fractionation** (Saturates, Aromatics, Resins, Asphaltenes), standardised as NF T 60-115 for asphaltene precipitation and Iatroscan chromatography (silica rod + flame ionisation detection) for the maltene fractions. **[5]**

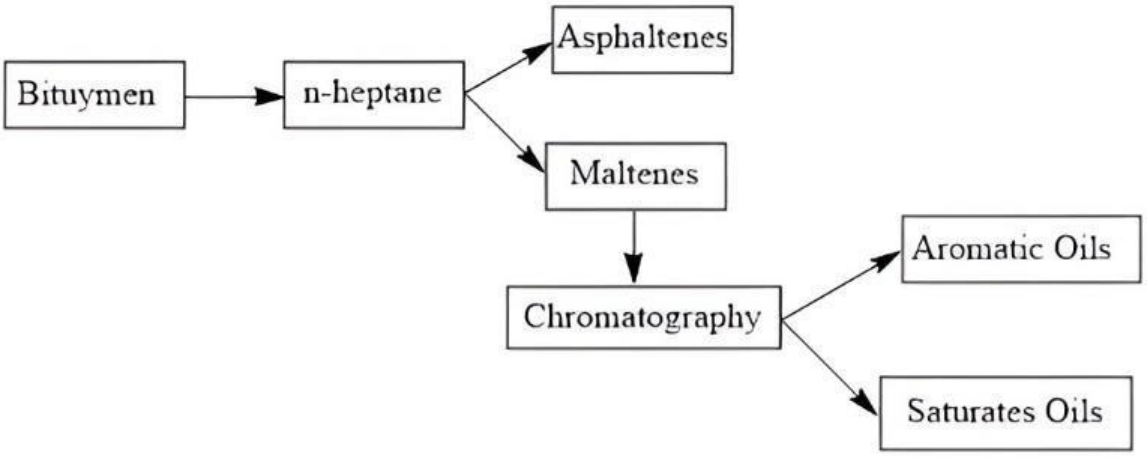
The first systematic fractionation was performed by Boussingault in 1837, who separated constituents by solubility in n-heptane, defining asphaltenes (insoluble) and maltenes (soluble). The four SARA fractions differ in molecular weight, polarity, and function within the colloidal microstructure:

The asphaltene fraction deserves particular attention. Asphaltenes are not individual molecules but nano-aggregates: aromatic sheets (4–10 rings) stack by π–π interactions into clusters approximately 2 nm in diameter, which further associate into aggregates 5–10 nm across. Their very high molar mass (up to 300 000 g/mol for aggregates) and strong polarity give bitumen its colloidal character. Transition metals (V,Ni) are incorporated as metalloporphyrins within asphaltene sheets.**[11]**

Table I.1: Comparative properties of the four SARA fractions of bitumen (compiled from).**[5]**

Fraction	Molar Mass (g/mol)	Content (%)	Key Characteristics
Saturates	300–800	5–15%	Linear, branched and naphthenic alkanes; non-polar; crystallisable waxes (10–15%); continuous oily phase
Aromatics	400–1500	40–65%	Mono-, di- and polycyclic aromatic rings + aliphatic chains; moderately polar; dispersing solvent for resins and asphaltenes
Resins	500–50 000	13–25%	Aromatic + naphthenic + heterocyclic rings (N, O, S); polar; act as peptisants stabilising asphaltene micelles
Asphaltenes	1 000–300 000	5–25%	Polycyclic aromatic sheets stacked by π–π interactions; very polar (N, O, S, metalloporphyrins); insoluble in n-heptane; colloidal dispersed phase

The **resins** are the molecular intermediaries between the polar asphaltenes and the non-polar aromatic–saturate matrix. They adsorb onto the asphaltene surface through polar interactions, forming a stabilising solvation shell. This role is called **peptisation**. It is this peptisation equilibrium that governs the colloidal stability of bitumen: any reduction in resin content (by oxidation) or change in aromatic/saturate ratio directly destabilises the system, leading to phase separation (Section 1.4).**[5]**



Schema I.2: Schematic of SARA fractionation (n-heptane precipitation of asphaltenes, then Iatroscan chromatography separating saturates, aromatics, and resins from the maltene fraction)

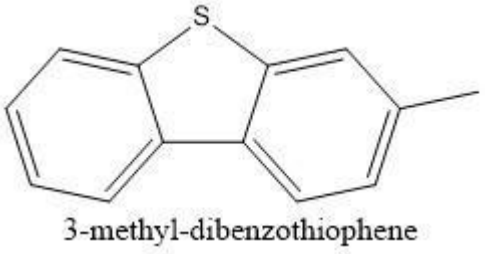


Figure I.3: Example of a resin chemical structure 3-methyl-dibenzothiophene ($C_{13}H_{10}S$).

I. 2.1: Colloidal Structure: Sol, Gel, and Sol-Gel

The SARA composition directly determines the colloidal microstructure of bitumen, which in turn governs all its macroscopic properties. Three structural types are distinguished: **[6]**

- **Sol structure ("island" model):** found in aromatic-rich bitumens with a high resin/asphaltene ratio. Asphaltene micelles are fully peptised and freely dispersed in the maltene phase. The material behaves as a nearly Newtonian viscous fluid, with low elasticity. This structure is stable but sensitive to volatilisation of aromatic maltenes.

- **Gel structure ("continental" model):** found in asphaltene-rich bitumens (blown bitumens). The high concentration of asphaltenes, insufficiently peptised by resins, leads to micelle agglomeration into a continuous three-dimensional network. The material exhibits marked elastic behaviour and high temperature susceptibility.
- **Sol-Gel structure:** the most common structure for road bitumens. The asphaltene aggregates are partially peptised by resins, forming clusters suspended in the maltene phase. The material is viscoelastic, exhibiting elastic behaviour at short time scales and low temperatures, and viscous behaviour at long time scales and high temperatures.

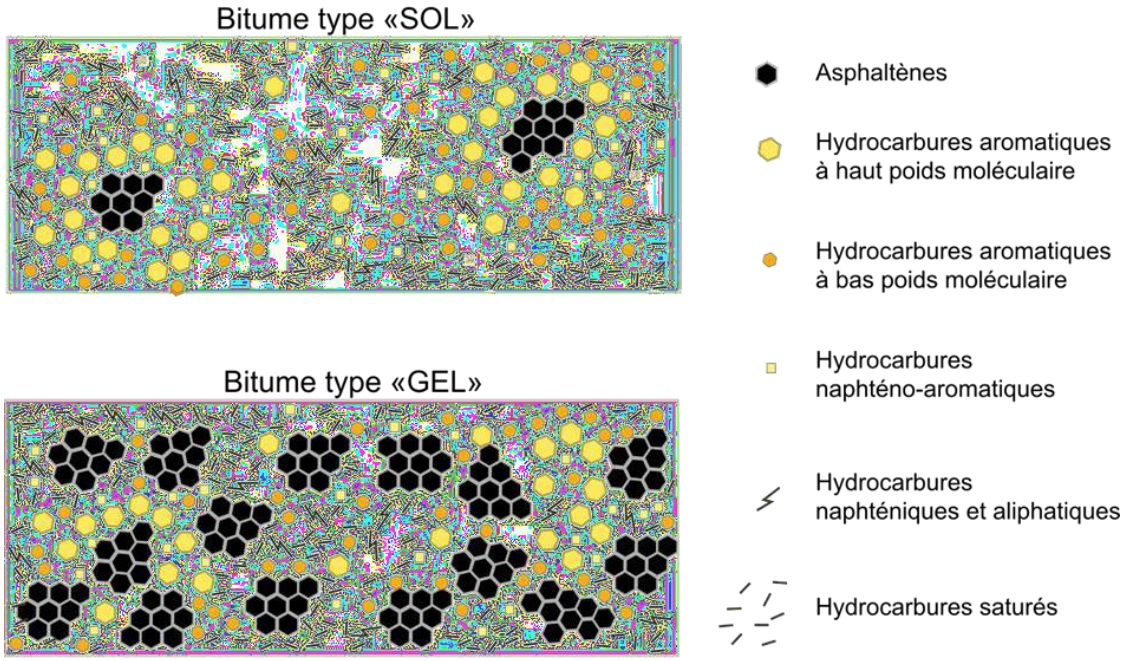


Figure I.4: Colloidal models of bitumen: Sol ("island") and Gel ("continental") structures, with Sol-Gel as the intermediate case for road bitumens.**[13]**

I. 3. Physicochemical Properties

The macroscopic properties of bitumen are a direct expression of its colloidal microstructure. Three properties are central to understanding both its use and its storage requirements.

I.3.1. Viscosity and Temperature Dependence

Viscosity is the most fundamental property of bitumen for storage and processing. Bitumen is a **non-Newtonian fluid** at ambient and low temperatures (viscosity depends on shear rate), but approaches Newtonian behaviour at the high temperatures used in storage and mixing (150–200°C).**[7]**

The viscosity–temperature relationship governs all handling operations. It is described by the **Walther–ASTM equation** ($\log \log \eta = A - B \log T$) or, in the framework of linear viscoelasticity, by the **Williams–Landel–Ferry (WLF) shift factor** used to construct the bitumen's master curve. Practically:

- At 25°C: bitumen is a semi-solid ($\eta \sim 10^5$–10^8 Pa·s depending on grade). Pumping is impossible.
- At 135°C: viscosity falls to 0.1–0.3 Pa·s, the threshold for mixing with aggregates (Brookfield viscometer, EN 13302).
- At 150–180°C: viscosity is typically 0.05–0.15 Pa·s, enabling efficient pumping and storage circulation.
- Above 200°C: accelerated oxidative degradation begins, causing irreversible hardening.

This narrow workable temperature window between 150°C (minimum pumpability) and 200°C (maximum thermal stability) is the fundamental reason why storage temperature control is critical.**[4]**

Measurement: the **Brookfield rotary viscometer** (EN 13302) measures dynamic viscosity at high temperatures (typically 60°C, 135°C, 165°C). The **Dynamic Shear Rheometer (DSR)** (EN 14770) measures the **complex modulus G*** (total stiffness, Pa) and the **phase** angle δ (0° = pure elastic solid; 90° = pure viscous liquid) under oscillatory shear at intermediate temperatures.

I.3.2. Softening Point and Thermal Sensitivity

The **Ring and Ball softening point (T_{naln}, EN 1427)** is the temperature at which a steel ball (3.5 g) sinks 25 mm through a bitumen disc held in a brass ring immersed in a water or glycerol bath. It characterises resistance to permanent deformation at high service temperatures. For road bitumens: T_{naln} = 46–58°C (grade-dependent). For blown bitumens: T_{naln} may exceed 80°C. **[4]**

The **Penetration Index (PI)**, calculated from penetration at 25°C and T_{naln}, quantifies temperature susceptibility:

$PI = (20 - 500 \times \log(pen/800)) / (1 + 50 \times \log(pen/800) \times 0.02 \times T_{naln})$.

A PI between −1 and +1 indicates a typical road bitumen; PI > +2 indicates a gel-type blown bitumen; PI < −2 indicates a highly temperature-susceptible sol-type bitumen.**[3]**

I.3.3. Thermal Stability

Thermal stability refers to the resistance of bitumen to irreversible chemical and physical changes under the combined action of heat and oxygen. It is characterised by two standardised ageing protocols that simulate the two phases of bitumen's service life: **[8]**

- **Short-term ageing (RTFOT, EN 12607-1):** Rolling Thin Film Oven Test, a thin rotating film of bitumen is exposed to 163°C air for 85 minutes, simulating the thermal and oxidative exposure during mixing and paving. Key indicator: mass loss (%) and change in penetration and softening point.
- **Long-term ageing (PAV, EN 14769):** Pressure Ageing Vessel RTFOT-aged bitumen is further aged at 100°C under 2.1 MPa of air pressure for 20 hours, simulating 5–10 years of in-service oxidation.

The primary indicator of thermal–oxidative degradation is the **carbonyl index (CI)**, measured by Fourier-Transform Infrared Spectroscopy (FTIR) as the area of the C=O absorption band (~1700 cm^{-1}). As CI increases, the bitumen becomes stiffer and more brittle, explaining why storage at excessive temperatures produces a non-compliant binder.**[8]**

I.3.4. Other Essential Properties

For completeness, the following properties are defined by the European standard EN 12591 for pure road bitumens:

Additional properties: adhesiveness (Vialit test, EN 12272-3), waterproofing (water absorption), and cold-temperature cracking resistance (Bending Beam Rheometer,

BBR, EN 14771, measuring creep stiffness S and relaxation rate mat −10°C and −20°C) complement the characterisation of bitumen for specific applications.**[4]**

Table I.2: Physicochemical specifications for road bitumens 35/50 and 50/70 according to EN 12591.

Parameter	Test Method	35/50	50/70	Physical Significance
Penetration at 25°C (0.1 mm)	EN 1426	35–50	50–70	Hardness/stiffness at ambient T
Ring & Ball softening point (°C)	EN 1427	50–58	46–54	Resistance to permanent deformation
Flash point (°C)	EN ISO 2592	≥ 230	≥ 230	Safety limit for storage heating
Kinematic viscosity at 135°C (mm^2/s)	EN 12595	≥ 370	≥ 295	Pumpability / mixing workability
Solubility in toluene (%)	EN 12592	≥ 99.0	≥ 99.0	Purity of binder
Mass loss after RTFOT (%)	EN 12607-1	≤ 0.5	≤ 0.5	Short-term thermal stability
Change in penetration after RTFOT (%)	EN 1426	≥ 53	≥ 50	Resistance to oxidative hardening

I. 4. Storage Problems

The requirement to maintain bitumen at 150–200°C for extended periods creates four interrelated categories of problem, each rooted in the physicochemical properties described above. Understanding this link is essential: storage problems are not arbitrary failures but predictable consequences of the bitumen's chemistry and colloidal structure.**[2]**

I.4.1. Oxidative Ageing

Oxidation is the dominant degradation mechanism during hot storage. Oxygen dissolved in the bitumen reacts with the aromatic and naphthenic components through a **free-radical chain reaction**: initiation produces peroxy radicals (ROO•); propagation converts maltene molecules into polar oxygenated species; termination forms stable products: **[8]**

- Carbonyl groups (C=O): ketones (~1700 cm^{-1} in FTIR) and carboxylic acids (~1700 cm^{-1}), measured by the Carbonyl Index (CI).
- Sulfoxide groups (S=O): formed by oxidation of thiophenic sulfur, contributing to polar crosslinking.
- Anhydrides and lactones: cross-linking products that stiffen the matrix.

The macroscopic consequence is well-defined: light maltenes (aromatics, saturates) are converted into heavy polar molecules resembling resins or asphaltenes. The penetration decreases, the softening point rises, and the bitumen becomes progressively more brittle and less workable. At storage temperatures (150–200°C), this reaction is significantly accelerated compared to in-service conditions, the rate approximately doubles for every 10°C increase (Arrhenius law).**[10]**

The carbonyl index measured by FTIR is the standard diagnostic tool:

- CI < 0.5 (arbitrary units): fresh, unaged bitumen.
- CI 0.5–2.0: moderate short-term ageing (equivalent to RTFOT).
- CI > 2.0: significant ageing; binder stiffness and brittleness substantially increased.

I.4.2. Phase Separation and Colloidal Instability

Phase separation during storage is a direct consequence of the oxidative degradation of **resins**, the peptisants of the colloidal system described in Section 1.2. As resins are oxidised into heavier, less soluble species, their ability to maintain the solvation shell
around asphaltene micelles is reduced. The colloidal equilibrium shifts from Sol-Gel toward Gel, and ultimately toward complete aggregation. The result is **sedimentation**: asphaltene aggregates settle to the tank floor while the lighter maltene phase rises to the surface.

The severity of this risk is quantified by the Colloidal Instability Index (CII)**:[15]**

CII = (Saturates + Asphaltenes) / (Aromatics + Resins)

- CII > 0.9: the resin/aromatic phase is insufficient to peptise the asphaltenes → high risk of sedimentation (Gel-type bitumen behaviour).
- 0.7 < CII < 0.9: intermediate stability; monitoring required during storage.
- CII < 0.7: stable system; asphaltenes are well-peptised (Sol-type bitumen).

The practical consequence is severe: after phase separation, the settled deposit is hard, non-pumpable, and chemically different from the surface layer. The binder's rheological properties are significantly altered, rendering it non-compliant with specifications and resulting in brittle asphalt mixtures in the field. Prevention requires continuous mechanical agitation and strict temperature control.

For polymer-modified bitumens (PMB), storage stability is assessed by the NF EN **13399 tube test**: the bitumen is stored vertically at 180°C for 3 days, then the tube is sectioned into thirds. A difference in Ring & Ball softening point between the top and bottom sections greater than 5°C indicates non-compliant polymer separation (creaming).

I.4.3. Thermal and Exudation Problems

- **Accelerated thermal degradation:** above 200°C, the oxidative ageing reactions described in Section 1.4.1 accelerate dramatically, causing rapid hardening and loss of penetration. ASTM and European standards require that storage temperature be maintained at a minimum of 30°C below the flash point (generally 230°C for pure bitumen).
- **Exudation (seepage) of maltenes:** under sustained heat, the lightest maltene fraction (low-viscosity aromatic oils) migrates to the surface or walls of the storage tank by capillary and thermal gradient effects. This selective loss of light components from the bulk bitumen accelerates its hardening locally, while the exuded oils significantly lower the local flash point, increasing fire and spontaneous ignition risk.

The flash point of the exuded oils can be as low as 60°C if a cutback-type solvent is present.

I.4.4. Corrosion by Naphthenic Acidity

Bitumen from certain crude sources contains significant quantities of naphthenic acids, characterised by the Total Acid Number (TAN, ASTM D664), which measures the quantity of KOH (mg) required to neutralise 1 g of bitumen. When TAN > 0.5 mg KOH/g, the bitumen is considered corrosive. At storage temperatures (150–200°C), naphthenic acids attack steel tank

walls through a chelation mechanism, dissolving the protective iron sulfide (FeS) layer and causing progressive wall thinning**. [2]**

Corrosion is most severe at the liquid/vapour interface (waterline) and on the heating elements, where the combination of acid concentration and

thermal stress is maximum.

I.4.5. Health, Safety, and Industrial Hazards

Hot bitumen storage presents significant occupational and industrial safety risks: **[9]**

- **Polycyclic Aromatic Hydrocarbon (PAH) vapours:** heating bitumen above 150°C generates aerosols and vapour containing PAHs, classified by the International Agency for Research on Cancer (IARC) as possibly carcinogenic (Group 2A). The occupational exposure limit for bitumen fumes (mineral fraction, aerosols, and vapour) is 5 mg/m³ in most international frameworks. Adequate ventilation and personal protective equipment are mandatory.
- **Fire and explosion:** the flash point of pure bitumen is ≥ 230°C. However, the flash point of exuded oils or cutback bitumens can be as low as 60–100°C. Flammable vapours accumulate in the headspace above the bitumen, creating an explosion risk. Storage temperature must always be maintained ≥ 30°C below the flash point.
- **Burn hazards**: liquid bitumen at 150–200°C causes severe deep burns on contact. During transfer and transport operations, spontaneous ignition of bitumen or associated vapours is a documented risk.
- **Water contamination: any** water ingress into a hot bitumen tank causes violent foaming and potential overflow (steam explosion). Water content must be kept below 0.2% (EN ISO 3733). Tanks must be thoroughly dried before filling.

I. 5. Chemical Solutions:

Additives to Improve Stability and Reduce Processing Temperature

The storage problems identified in Section 1.4, oxidative ageing, colloidal phase separation, thermal exudation, and naphthenic corrosion, are not inevitable. Each has a targeted chemical solution in the form of additives incorporated into the bitumen formulation.

Four main families are distinguished according to their primary function: antioxidants, which interrupt the free-radical oxidation chain responsible for hardening; polymeric modifiers, which reinforce the colloidal network and limit phase separation during storage fluxing agents and bio-based softeners, which reduce viscosity and lower the minimum handling temperature;

and warm mix additives (WMA), which allow mixing and compaction temperatures to be reduced by 30–50°C relative to conventional hot mix asphalt, directly limiting thermal ageing during production.**[10]**

The selection of an appropriate additive or combination of additives depends on four interdependent criteria: chemical compatibility with the bitumen and SARA composition, technical efficiency under storage and service conditions, long-term stability without inducing secondary degradation, and economic viability at an industrial scale. These criteria, and the detailed mechanisms by which each additive family acts on the bitumen and physicochemical properties, are examined systematically in Chapter II.

Conclusion

This chapter presents a mechanistic understanding of bitumen, characterising it as a colloidal system influenced by the peptisation equilibrium between resins and asphaltenes. The viscosity–temperature relationship necessitates storing bitumen between 150°C and 200°C to prevent pump failure and oxidative degradation. This temperature range contributes to storage issues such as oxidative ageing, colloidal phase separation, thermal exudation, and naphthenic acid corrosion. Additive solutions are aligned with specific problems: antioxidants counteract oxidation, sulfur-vulcanised SBS stabilises phases, bio-based softeners lower viscosity safely, and synthetic waxes enhance the matrix. The next chapter will explore the properties of these additives and their impact on bitumen performance and stability.

References

[1] Read, J., & Whiteoak, D. (2003). The shell bitumen handbook. Thomas Telford.

[2] Lesueur, D. (2009). The colloidal structure of bitumen: Consequences on the rheology and on the mechanisms of bitumen modification. Advances in colloid and interface science, 145(1-2), 42-82.

[3] Redelius, P., & Soenen, H. (2015). Relation between bitumen chemistry and performance. Fuel, 140, 34-43.

[4] EN12591, H. R. N. (2009). Bitumen and Bituminous binders—specifications for paving grade bitumens. CEN: Brussels, Belgium.

[5] Mullins, O. C., Sheu, E. Y., Hammami, A., & Marshall, A. G. (2007). Asphaltenes, heavy oils, and petroleomics. Springer Science & Business Media.

[6] Loeber, L., Sutton, O., Morel, J. V. J. M., Valleton, J. M., & Muller, G. (1996). New direct observations of asphalts and asphalt binders by scanning electron microscopy and atomic force microscopy. Journal of microscopy, 182(1), 32-39.

[7] Ferry, J. D., & Myers, H. S. (1961). Viscoelastic properties of polymers. Journal of The Electrochemical Society, 108(7), 142C-143C.

[8] Petersen, J. C. (2009). A review of the fundamentals of asphalt oxidation: chemical, physicochemical, physical property, and durability relationships. Transportation research circular, (E-C140).

[9] Mundt, K. A., Dell, L. D., Crawford, L., Sax, S. N., & Boffetta, P. (2018). Cancer risk associated with exposure to bitumen and bitumen fumes: an updated systematic review and meta-analysis. Journal of Occupational and Environmental Medicine, 60(1), e6-e54.

[10] Polacco, G., Filippi, S., Merusi, F., & Stastna, G. (2015). A review of the fundamentals of polymer-modified asphalts: Asphalt/polymer interactions and principles of compatibility. Advances in colloid and interface science, 224, 72-112.

[11] Mullins, O. C., Sabbah, H., Eyssautier, J., Pomerantz, A. E., Barré, L., Andrews, A. B., ... & Zare, R. N. (2012). Advances in asphaltene science and the Yen–Mullins model. Energy & Fuels, 26(7), 3986-4003.

[12] ABABSA Moussira: "Valorization of bitumen-polymer mixtures by the pyrolysis process", Master's thesis defense, defended on 29/01/2006, Materials Chemistry p 3-11 (CU Larbi Ben M'hidi Oum Elbaouaghi)

[13] KAMASSI, N. (2019) Highly polymer-modified bitumen (HIMA): influence of polymers on binder viscosity ─ Case study: D0234. Master's thesis.

Kasdi Merbah University. Ouargla.

Chapter II:

Bitumen Stabilising Additives.

Introduction

Bitumen, a viscous and impermeable thermoplastic material, is the basic binder for almost all asphalt mixes used in road construction. Its industrial application, particularly the storage, pumping, and coating of aggregates, conventionally requires temperatures between 160 and 200°C. These harsh thermal conditions generate several cumulative problems: high-energy consumption, emissions of harmful bituminous fumes, safety risks for operators, and accelerated oxidative ageing of the binder.

The introduction of specific additives into bitumen formulations constitutes a technological response to these challenges. By modifying viscosity, colloidal stability, or oxidation resistance, these additives enable acceptable rheological performance at significantly reduced storage and application temperatures (130–140 °C) within the framework of Warm Mix Asphalt (WMA) technology. **[1,2]**

This chapter presents the mechanisms of action of stabilising additives, their classification, the relevant selection criteria, as well as the justification for the choice of the three additives retained in the context of this work.

II. 1. General role of additives in bitumen

The additives incorporated into bitumen can be grouped into three main functional categories, directly linked to the degradation mechanisms to which the binder is subjected during high-temperature storage: **[3,5]**

II.1.1. Antioxidants

Antioxidants delay or inhibit the radical oxidation reactions that progressively degrade the aromatic and resin fractions of bitumen. They act either by scavenging free radicals (hydrogen-donating mechanism) or by decomposing the hydroperoxides formed. Hindered phenolic antioxidants, such as 2,6-di-tert-butylphenol, are the most common representatives of this family.**[14]**

II.1.2. Thermal stabilisers

Thermal stabilisers maintain the chemical and rheological integrity of the binder during prolonged heating cycles (storage at 140–200 °C).**[4]**

They limit the formation of oxidation products (carbonyls, sulfoxides) that stiffen the bitumen. Some polymers, such as EVA and SBS, fall into this category due to their excellent thermal stability up to 180–200 °C. **[7]**

II.1.3. Dispersing agents and viscosity modifiers

These additives act on the colloidal structure of bitumen by improving the dispersion of asphaltene micelles in the maltenic phase. By reducing intermolecular interactions, they lower the viscosity of the binder at a given temperature, thus facilitating the wetting of aggregates at lower application temperatures. Fischer- Tropsch waxes (Sasobit) and certain aromatic amides illustrate this category.**[8]**

II. 2. Mechanisms of action

II.2.1. Free radical inhibition

The oxidation of bitumen follows a chain radical kinetics whose three stages are:

- Initiation: RH + O_2 → R• + HOO• (thermal or photochemical initiation)
- Propagation: R• + O_2 → ROO•; ROO• + RH → ROOH + R• (self-sustaining cycle)
- Termination: R• + R• → R–R; ROO• + ArOH → ROOH + ArO • (intervention of the antioxidant)

Phenolic antioxidants interrupt the propagation cycle byproviding a hydrogen atom to peroxide radicals according to the reaction:

ROO• + ArOH → ROOH + ArO • (ArO •: resonance-stabilised phenoxyl radical).**[3]**
phenoxyl radical ArO • is relatively unreactive due to electron delocalisation on the aromatic ring and the steric effects of the tert -butyl groups in the ortho position, which prevents reinitiation of the oxidative chain. This mechanism is the basis for the choice of 2,6-di-tert-butylphenol in this work (see section 2.5). **[3,14]**

II.2.2. Stabilisation of asphaltenes

Bitumen is a colloidal system in which asphaltenes, a high molar mass polyaromatic fraction (1000–3500 g/mol), form resin-stabilised micelles. During thermal or oxidative ageing, this colloidal system becomes destabilised by progressive agglomeration of the micelles, leading to phase separation. **[5,6]**

The stabilising additives in asphaltenes act through two complementary mechanisms:

- **Hydrogen bond (H-bond)** type interactions between the polar functional groups of the additive (amide, acid, phenol) and the N, S, O heteroatoms of asphaltenes, increasing their compatibility with the maltenic phase.
- **polyaromatic rings of asphaltenes**, promoting the dispersion of aggregates (peptization). **[5,6]**

II. 2.3. Improved fluidity and reduced implementation temperature

The viscosity of bitumen, governed by intermolecular interactions between asphaltenes and between asphaltenes and maltenes, can be temporarily reduced by viscosity-modifying additives. Two mechanisms are involved: **[5]**

- **Physical mechanism (waxes):** Long-chain waxes (C_{45}–C_{100}, Sasobit type) are miscible in bitumen above their melting point (~100 °C), reducing viscosity through a plasticising effect. Below this threshold, they crystallise and mechanically strengthen the binder.**[8]**

- **Surfactant mechanism (chemical additives):** amphiphilic molecules (aromatic amides, esters) adsorb at the asphaltene- maltene interface, reducing intermolecular friction forces and improving the wetting of aggregates at reduced temperature. **[1,2]**

WMA technology exploits these mechanisms to produce asphalt at 110–140 °C instead of 160–190 °C, a reduction of 20 to 50 °C.

II.3. Classification and examples of additives used in industry

Table II.1: presents a cross-classification of the main industrial additives according to their function and area of application: **[2,5]**

Family	Mechanism	industrial example	Dosage/effect
Phenolic antioxidants	Radical inhibition (H-donor)	Irganox 1010 / BHT (Oil Tanker)	0.1–1%; ↑ILO 30–50%
Amino antioxidants	Radical trapping (N-donor)	N-phenyl-naphthylamine (Road)	0.5–2%; UV anti-aging

Waxes FT (WMA)	Plasticization, ↓ viscosity T > Tf	Sasobit ® C45–C100 (Road)	2–4%; ΔT = −20 to −40 °C
Aromatic amides	Asphaltene dispersant (H-bond + π – π)	Rediset® WMX (Road)	0.2–0.5%; anti-pull
Polymer modifiers (SBS/EVA)	Elastic network/stiffening	SBS (BMP NAFTAL 10-40/70)	3–6%; ↑ Tf ≥ 70 °C

II.4. Criteria for selecting additives

The choice of an additive for the formulation of a modified bitumen is based on four complementary criteria, the weighting of which depends on the intended application:

II.4.1. Functional efficiency

Efficacy is measured by tests specific to each mechanism of action:

- Antioxidants: oxidation induction time (OIT, ASTM E1641), O–H bond dissociation energy (BDE, calculable by DFT), resistance to ageing RTFOT/PAV. **[9,10,11]**
- Dispersants: storage stability (EN 13399), colloid index (Uf), variation in penetrability before/after ageing.[12]
- Viscosity modifiers: measurement of dynamic viscosity at 135 °C (EN 13302), reduction of compaction temperature (target ΔT ≥ 20 °C**).[13]**

II. 4.2. Thermal stability

The additive must withstand mixing (130–160 °C) and storage (140–200 °C) temperatures without decomposition. The decomposition start temperature (Td, ATG/TGA) must be at least 30 °C higher than the service temperature. SBS and EVA polymers have Td > 250 °C; bulky phenols such as 2,6-di-tBu-phenol have Td ≈ 260 °C. **[7]**

II. 4.3. Compatibility with bitumen

Chemical compatibility is governed by solubility parameters (Hildebrand factor) and the polarity of the additive. Insufficient compatibility leads to phase separation during storage, as assessed by the EN 13399 storage tube test (ΔTf ≤ 5 °C acceptable).

Aromatic additives are generally compatible with the aromatic and resin fractions of bitumen. **[5,12]**

II.4.4. Cost and availability in the Algerian context

In the Algerian industrial context (NAFTAL, ENR), the local availability of precursors is a determining factor. Phenol (precursor of 2,6-di-tBu-phenol) and aniline (precursor of N-phenyl-benzamide) are industrially available chemicals in Algeria. This criterion justifies the choice of laboratory synthesis rather than the purchase of imported commercial additives.

II.5. Choice and justification of the additives used in this work

The selection of the three additives is based on a complementary strategy covering the three main mechanisms of 70/100 bitumen degradation during high-temperature storage:

II.5.1. Additive 1: 2,6-di-tert-butylphenol Primary antioxidant

sterically hindered phenol by two tert-butyl groups at positions 2 and 6. Molar mass = 206 g/mol. Melting point = 35–37 °C.

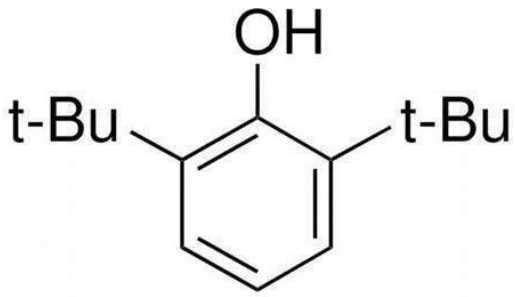


Figure II.1: chemical structure of 2, 6-di-tert-butylphenol.

Hydrogen Atom Transfer) type antioxidant activity. The two tert -butyl substituents in the ortho position stabilize the phenoxyl radical. ArO
formed after hydrogen donation, thus interrupting the oxidative chain. The aromaticity of the molecule ensures its compatibility with the aromatic fractions of 70/100 bitumen (45–60%) and facilitates its interaction with the polyaromatic rings of asphaltenes by π–π stacking. **[3,14]**

Expected mechanism in DFT: calculation of the O–H BDE (O–H bond dissociation energy, correlated with antioxidant activity), HOMO-LUMO gaps, and interaction energies with coronene (asphaltene model).

Industrial analogy: 2,6-di-tert-butylphenol is the basic molecule of BHT (Irganox, Lowinox), a reference antioxidant for polymers and industrial oils.

II.5.2. Additive 2: N-phenyl-benzamide (benzanilide) Colloidal stabiliser

Structure: Aromatic amide formed by the condensation of aniline and benzoyl chloride. Molar mass = 197 g/mol. Melting point = 163 °C.

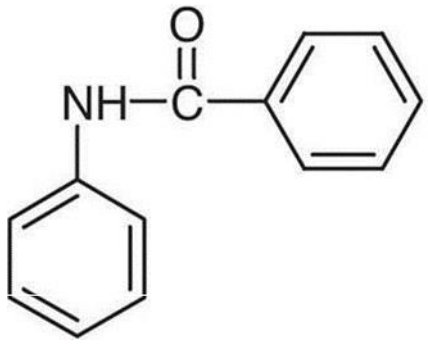


Figure II.2: chemical structure of N-pheny-lbenzamide

Justification: The molecule possesses two distinct functionalities that allow for multiple interactions with the components of bitumen: (1) the polar amide group (C=O, N–H) forms hydrogen bonds with the nitrogen and sulfur groups of the resins and asphaltenes; (2) the two phenyl rings form π–π interactions with the polyaromatic rings of the asphaltenes. This dual interaction promotes the peptization of asphaltene micelles and improves the system's colloidal stability. **[5,6]**

Expected mechanism in DFT: calculation of interaction energies with benzoic acid (resin model) and coronene, NBO analysis of charge transfers, and AIM topology of hydrogen bonds.

II.5.3. Additive 3: Benzyl benzoate Viscosity modifier/plasticiser

Structure: Aromatic ester produced by esterification of benzoic acid and benzyl alcohol.
Formula $C_{14}H_{12}O_2$, Molar mass = 212 g/mol. Colourless liquid, nD = 1.568.

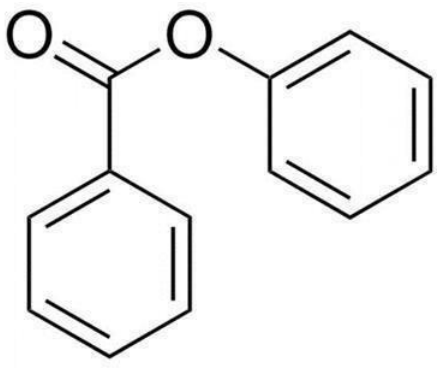


Figure II.3: chemical structure of Benzyl benzoate.

Rationale: The ester group increases the free volume of the bituminous matrix by reducing interactions between the molecular chains of saturated and low-molecular-weight aromatics.

This plasticising effect improves the molecular mobility of the system and reduces the apparent viscosity of the binder, thereby facilitating the wetting of aggregates at lower temperatures. The expected temperature reduction is on the order of 10–15 °C (plasticising effect alone), complementing the stabilising action of Additives 1 and 2. **[2,5]**

Expected mechanism in DFT: calculation of van der Waals interactions with squalane (saturated bitumen model), analysis of solubility parameters, and verification of miscibility in the bituminous system.

II.5.4. Expected synergy of the three additives

Table II.2: Summarises the complementarity of the three additives with respect to the degradation mechanisms of 70/100 bitumen:

Degradation mechanism	**Additive 1 (2,6-tBu₂PhOH)**	**Additive 2 (Benzanilide)**	**Additive 3 (Benzyl Benzoate)**
Radical oxidation	(H- donor)	(partial)	–
Asphaltene agglomeration	(π–π)	(H-bond + π–π)	–
Excessive viscosity	–	(partial)	(plasticiser)
Temperature reduction (ΔT)	-5 to -10 °C	-5 to -10 °C	-10 to -15 °C
Thermal stability (Td)	> 260 °C ✓	> 200 °C ✓	~200 °C ✓

Conclusion

This chapter presents the theoretical framework and chemical rationale for selecting three additives: hindered phenolic antioxidants, polar aromatic amides, and mobile esters. These chemically distinct families synergistically address degradation processes in 70/100 bitumen during high-temperature storage. The combination is expected to lower storage and application temperatures by 20 to 40 °C, shifting from 160–200 °C to the 130–140 °C range associated with WMA technology, while maintaining key rheological properties. Molecular modelling using DFT/PM7 will quantify atomic interactions and validate these choices computationally.

References

[1] Hurley, G. C., & Prowell, B. D. (2005). Evaluation of Aspha-Min zeolite for use in warm mix asphalt. NCAT report, 05-04.

[2] d'Angelo, J., Harm, E., Bartoszek, J., Baumgardner, G., Corrigan, M., Cowsert, J., ... & Yeaton, B. (2008). Warm-mix asphalt: European practice.

[3] Petersen, J. C. (2009). A review of the fundamentals of asphalt oxidation: chemical, physicochemical, physical property, and durability relationships. Transportation research circular, (E-C140).

[4] Airey, G. D. (2003). State of the art report on ageing test methods for bituminous pavement materials. International Journal of Pavement Engineering, 4(3), 165-176.

[5] Lesueur, D. (2009). The colloidal structure of bitumen: Consequences on the rheology and on the mechanisms of bitumen modification. Advances in colloid and interface science, 145(1-2), 42-82.

[6] Mullins, O. C., Sabbah, H., Eyssautier, J., Pomerantz, A. E., Barré, L., Andrews, A. B., ... & Zare, R. N. (2012). Advances in asphaltene science and the Yen–Mullins model. Energy & Fuels, 26(7), 3986-4003.

[7] Lu, X., Isacsson, U. L. F., & Ekblad, J. (2003). Influence of polymer modification on low temperature behaviour of bituminous binders and mixtures. Materials and Structures, 36(10), 652-656.

[8] Hurley, G. C., & Prowell, B. D. (2005). Evaluation of Sasobit for use in warm mix asphalt. NCAT report, 5(6), 1-27.

[9] Cardoso, E. C. L., Scagliusi, S. R., & Lugão, A. B. (2017). Gamma-radiation effect on biodegradability of synthetic PLA structural foams PP/HMSPP based. In Characterization of Minerals, Metals, and Materials 2017 (pp. 111-119). Cham: Springer International Publishing.

[10] Blab, R., Ahmad, J., Shaffie, E., Sidek, N., Mirwald, J., Eberhardsteiner, L., & Hofko, B. (2024). Performance of Crumb Rubber Tire-Modified Bitumen for Malaysian Climate Regions. Materials, 17(23), 5800.

[11] Test, O. (2012). Accelerated aging of asphalt binder using a pressurized aging vessel (PAV).

[12] Zani, L., Giustozzi, F., & Harvey, J. (2017). Effect of storage stability on chemical and rheological properties of polymer-modified asphalt binders for road pavement construction. Construction and building materials, 145, 326-335.

[13] EN, C. (2018). 13302: 2018; Bitumen and bituminous Binders—Determination of Dynamic Viscosity of Bituminous Binder Using a Rotating Spindle Apparatus. European Committee for Standardization: Brussels, Belgium, 16.

[14] Espinosa Ruiz, L. V. (2020). Analysis of bio-binders for paving as a total substitute for asphalt binder (Doctoral dissertation, Universidade de São Paulo).

Chapter III:

Foundations of Molecular Modelling

Introduction

Molecular modelling is an essential theoretical tool for studying complex systems in chemistry, particularly petroleum systems such as bitumen. It enables the description of molecules at the atomic scale and the analysis of their interactions using the principles of quantum chemistry and molecular mechanics. In the case of bituminous materials, this approach is particularly useful due to their highly heterogeneous nature and the difficulty of experimentally characterising all the interactions that govern their physicochemical properties.

In this work, we combine molecular dynamics (MD) to explore spatial configurations and temporal properties at the nanoscale, and density functional theory (DFT) for quantum-mechanical analysis of electronic interactions and reactivity quantities. This hybrid MD/DFT approach, now common in recent literature, allows us to couple conformational exploration with the electronic precision necessary to quantify the weak interactions that govern the cohesion of bituminous systems. Molecular modelling thus allows us to better understand the system's stability, the behaviour of heavy fractions, and the role of additives at the microscopic scale.**[8]**

III.1. The value of molecular modelling for bituminous systems

Bitumen is a complex material composed of a set of molecules belonging to different chemical families. This complexity makes a complete experimental description of its internal interactions difficult. Molecular modelling simplifies this complexity by representing the constituents of bitumen with model molecular structures. It thus offers the possibility of studying:

- The interactions between the different fractions of bitumen.
- The behaviour of heavy aromatic fractions.
- The mechanisms of molecular aggregation.
- The interactions between additives and the bituminous matrix.
- The influence of microscopic interactions on macroscopic properties.

In bituminous systems, rheological properties and stability depend strongly on intermolecular interactions. The main interactions involved are, in descending order of importance:

1. π–π interactions between aromatic systems: dominant forces in the packing of polyaromatic nuclei in asphaltenes.

2. Van der Waals forces: major contributions to cohesive energy, particularly between peripheral alkyl chains.

3. Hydrogen bonds: involving heteroatoms (O, N, S) present in resins and asphaltenes.

4. Electrostatic interactions: between polar groups.

π–π interactions and hydrogen bonds are also crucial for asphaltene aggregation, with a comparable contribution to nanoaggregate stabilisation. These authors showed by DFT calculations (ωB97X-D/6-31G (d, p)) that water bridges between heterocyclic dimers significantly enhance aggregation via cooperative interactions, with the stabilisation energy reaching −34.4 kcal/mol for pyridine dimers bridged by two water molecules. The theoretical analysis of these interactions allows for a better understanding of the mechanisms responsible for the cohesion of bitumen and its evolution over time, particularly under the effect of oxidative ageing.**[4]**

III. 2. Molecular representation of bitumen

III.2.1. SARA Approach

Bitumen is generally described according to the SARA classification, which distinguishes four main fractions based on their increasing polarity and molecular weight:

- **Saturates**: low-polarity aliphatic hydrocarbons responsible for the system's fluidity.
- **Aromatics:** compounds containing benzene rings, playing a role in the solvation of the heavier fractions.
- **Resins:** polar molecules containing heteroatoms (O, N, S), ensuring the system's stability through interaction with asphaltenes.
- **Asphaltenes**: the heaviest and most polar fraction, responsible for the structure and rigidity of bitumen.s classification, derived from standardised chromatographic separation (ASTM D4124), simplifies the study of bitumen by grouping its constituents according to their chemical properties and physicochemical behaviour. However,should be noted that this separation is An operational method that does not necessarily reflect the intrinsic molecular properties. Recent work shows that SARA fractions evolve significantly under oxidative ageing, affecting the rheological properties of the binder. Molecular modelling makes it possible to track these changes by quantifying the modifications of intermolecular interactions during ageing. **[6]**

III.2.2. Representation of asphaltenes

Asphaltenes are complex structures composed primarily of condensed aromatic rings and alkyl chains. They play a central role in the stability of bitumen. Historically, two structural models have been proposed to describe their molecular architecture:

a) Continental (or "island") model: this corresponds to a structure dominated by an extended central aromatic ring, surrounded by peripheral alkyl chains.

b) Archipelago model: this consists of several aromatic rings linked together by aliphatic chains. However, these models have been largely superseded in recent literature by the Yen-Mullins model (also called the modified Yen model), which is now the dominant reference framework.**[7]** According to this model:

- The most probable molecular mass of asphaltenes is approximately 750 g/mol.
- The "island" type molecular architecture (a single aromatic ring per molecule) is dominant.
- At sufficient concentrations, asphaltene molecules form nano-aggregates with fewer than 10 molecules, exhibiting a disordered arrangement of aromatic rings.
- At higher concentrations, the nano-aggregates form clusters again with a small number of units (< 10).

The size of the nano-aggregates has been experimentally determined to be approximately 2 nm by atomic force microscopy (AFM) of Langmuir-Blodgett films, while the clusters reach approximately 5 nm. **[5]**

This hierarchical model has been validated by a multitude of experimental techniques (SANS neutron scattering, SAXS X-ray scattering, DC conductivity, mass spectrometry) and forms the basis of the first predictive equation of state for asphaltene gradients in petroleum reservoirs (FHZ EoS).

III.2.3. Model Molecules

To represent the different fractions of bitumen in theoretical studies, simplified molecules are often used. This approach allows the study of fundamental interactions without resorting to the full complexity of real bitumen. Model molecules commonly used in recent literature include:

- Saturates: model aliphatic hydrocarbons (n-octane, n-dodecane, squalene).
- Aromatics: simple benzene systems (benzene, naphthalene, anthracene, pyrene).
- Resins: heterocyclic molecules (pyridine, thiophene, furan, isoquinoline, carbazole).

- Asphaltenes: condensed polyaromatic structures such as the PBP (4,4′-bis(2-pyren-1-yl-ethyl) 0-2,2′-bipyridine) model proposed by Grey et al., validated experimentally and by DFT to simulate the aggregation behaviour of asphaltenes**. [2]**

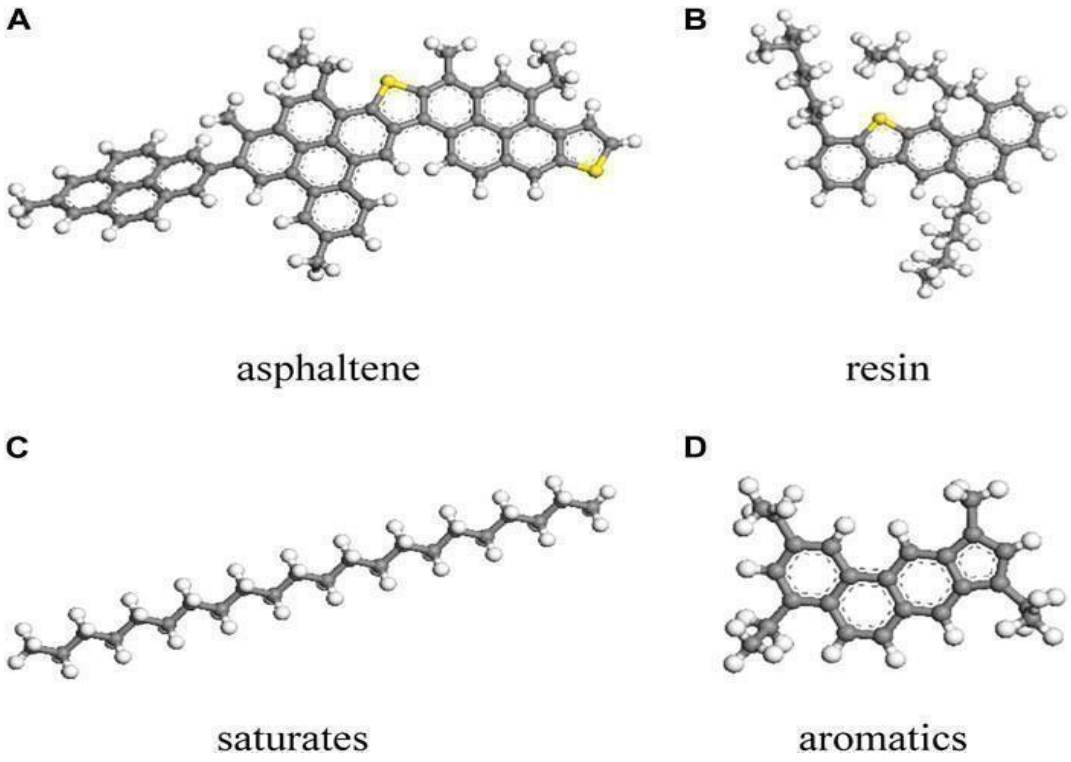


Figure III.1: Representation Schematic of the SARA fractions of bitumen and corresponding model molecules: **(a)** saturated (aliphatic hydrocarbons), **(b)** aromatic (benzene rings), **(c)** resins (polar heterocyclic molecules), **(d)** asphaltenes (condensed island-type polyaromatic structures according to the Yen-Mullins model).

III.3. Principles of molecular modelling methods:

III.3.1. Geometric Optimisation:

Geometric optimisation involves determining the most stable spatial configuration of a molecule, corresponding to a minimum of potential energy on the hyperspatial energy surface. This process relies on finding the most thermodynamically stable structure by adjusting atomic positions until energy gradients converge (typically < 0.001 Hartree/Bohr). For bituminous systems, geometric optimisation is an essential preliminary step before any calculation of electronic properties or molecular dynamics.

III.3.2. Semi-empirical methods

Semi-empirical methods are based on the principles of quantum mechanics but incorporate parameters from experimental data to reduce computational complexity. They allow for a rapid and approximate description of molecular systems, particularly useful for large structures or for preliminary exploration of the potential energy surface. Methods such as PM6, PM7, or tight-binding methods (DFTB) are sometimes used for large bituminous systems, although their accuracy for weak interactions remains limited.

III.3.3. Density Functional Theory (DFT)

DFT is a fundamental quantum method for describing the electronic properties of molecular systems based on the electron density ρ(r), rather than the multi-electron wavefunction. It is now one of the most widely used approaches for studying complex molecular systems. It provides access to essential information such as:

- Total electron energy.
- Electron density distribution.
- Chemical reactivity (frontier orbitals, reactivity indices).
- The nature of intermolecular interactions.

This method is particularly well-suited to studying weak interactions such as dispersion and π–π interactions, provided that appropriate functionals are used. Indeed, standard functionals such as LDA (Local Density Approximation) or GGA (Generalised Gradient Approximation, PBE, BLYP) systematically underestimate dispersion interactions, making them unsuitable for the quantitative study of π–π packing in asphaltenes**.[9]**

For bituminous systems, the following functionals are recommended:

Table III.1: Recommended DFT functionals for the study of bituminous systems.

Functional	Kind	Main advantage	Bitumen application
ωB97X-D	Hybrid + dispersion	Excellent for π–π and H-bridges	Model asphaltene dimers (Lessa et al.2024)
B3LYP-D3	Hybrid + Grimme correction	Good compromise between accuracy and cost	Asphaltene porphyrin interactions

M06-2X	Meta functional	Effective for non-covalent interactions	Molecular aggregation
BLYP-D3	GGA + dispersion	Economical for large systems	Preliminary geometric optimization

The work of Stoyanov et al. (2012), widely cited and validated in recent literature, demonstrated the effectiveness of the ωB97X-D functional associated with the 6-31G (d, p) basis to quantify the respective contributions of π–π stacks and hydrogen bridges in the aggregation of model asphaltenes.

III.3.4. Basic Sets

Base sets provide a mathematical representation of atomic orbitals in quantum calculations. They allow the electronic distribution of molecules to be described with varying degrees of accuracy depending on the size of the chosen basis. The classical hierarchy includes:

- Minimal bases (STO-3G): insufficient for weak interactions.
- Double-sized bases (6-31G, 6-311G): standard for geometry.
- Polarised bases (6-31G (d, p), 6-311G (d, p)): necessary to capture electronic polarisation in interactions.
- Diffuse bases (aug-cc-pVDZ, aug-cc-pVTZ): essential for anions and long-range interactions.

For studies of intermolecular interactions in bituminous systems, the use of polarised bases is recommended. In addition, the interaction energy must be corrected for the base set superposition error (BSSE) by the Boys and Bernardi counterpoise method, especially for weak interactions where this correction can reach 20–30% of the gross energy.

III.3.5. Functionalities of the DFT

DFT functionals play a central role in the accuracy of electronic calculations. They allow us to describe the exchange and correlation energies of electrons. We distinguish between:

1. Local functionals (LDA, GGA: PBE, BLYP): fast but underestimate dispersion.
2. Hybrid functionals (B3LYP, PBE0, ωB97X): include an exact exchange term (fraction of Hartree-Fock orbitals), better for electronic properties and the activation barrier.

3. Functionals with dispersion correction (ωB97X-D, B3LYP-D3, M06-2X, BLYP-D3): essential for bituminous systems because they accurately capture van der Waals interactions and π–π stacking.

Some functionals are particularly well-suited to the study of organic systems and weak interactions, especially those involving dispersion and aromatic systems. The choice of the functional must be validated by comparison with experimental data or reference methods (coupled-cluster CCSD(T)) on model systems.

III.3.6. Molecular Dynamics (MD)

Molecular dynamics is an essential complement to DFT for exploring temporal properties and spatial configurations at the nanoscale. Unlike DFT, which provides a static image of the energy minimum, MD allows us to:

- explore the potential energy surface at a finite temperature.
- calculate transport properties (viscosity, diffusion).
- track the temporal evolution of asphaltene aggregation.
- study the effects of ageing and additives. For bituminous systems, two force field approaches are primarily used:
- All-atom (AA) force fields: very accurate but expensive for large systems.
- United-atom (UA) force fields: group hydrogen atoms with their parent atom, reducing the number of particles by a factor of approximately 2 and accelerating simulations by 10 to 100 times. Assaf et al. (2024) recently developed a force-matching AU force field based on an all-atom model, allowing MD simulations to be extended to larger spatiotemporal scales while preserving the fidelity of structural and thermodynamic properties (pressure, density, morphology).

III. 4. Theoretical quantities used in molecular modelling

III.4.1. Interaction Energy

Interaction energy allows us to quantify the stability of a molecular complex formed between two chemical entities, A and B:

$$\Delta E_{int} = Complex - (E_A + E_B)$$

A negative value indicates a stabilising interaction between molecular species. As mentioned previously, the BSSE (Basis Set Superposition Error) correction is essential to obtain physically significant interaction energies, particularly when moderately sized bases are used. For a more detailed analysis, the interaction energy can be decomposed according to Energy Decomposition Analysis (EDA) into electrostatic, polarisation, exchange, dispersion, and Pauli repulsion contributions. For hydrogen bonds in heterocyclic phthalein dimers, the polarisation and exchange (partial covalent character) terms contribute approximately 80% of the total stabilisation energy, while dispersion dominates in pure π–π stacks. **[4]**

III.4.2. HOMO and LUMO frontier orbitals

Frontier orbitals play a fundamental role in chemical reactivity. The HOMO–LUMO energy gap is defined by:

$$\Delta E_{gap} = E_{LUMO} - E_{HOMO}$$

A small energy gap generally indicates high chemical reactivity and low electronic stability. However, the HOMO–LUMO gap alone is insufficient to predict reactivity in complex bituminous systems. More sophisticated reactivity indices are commonly used:

- Chemical potential: $\mu = \frac{E_{HOMO}+E_{LUMO}}{2}$
- Chemical hardness: $\eta = \frac{E_{LUMO}-E_{HOMO}}{2}$
- Electrophilicity: $\omega = \frac{\mu^2}{2\eta}$
- Sofnesse: $S = \frac{1}{2\eta}$
- Fukui indices: locate reactive sites on atoms.

  $f_k^+ = q_k(N+1) - q_k(N)$

  $f_k^- = q_k(N) - q_k(N-1)$

These quantities, accessible by DFT, allow for the rationalisation of the reactivity of different SARA fractions in the face of oxidative ageing or interactions with additives.

III.4.3. Electron density

Electron density describes the distribution of electrons within a molecule, enabling the identification of electron-rich or electron-deficient regions. It is an essential tool for understanding reactive sites and intermolecular interactions. Analysis of electron density using quantum topology tools (QTAIM: Quantum Theory of Atoms in Molecules) allows the characterisation of the nature of bonds and interactions (covalent, ionic, weak).

III.4.4. Weak intermolecular interactions

Weak interactions play a crucial role in the cohesion of bituminous systems. They primarily include:

- **π–π interactions**: the stacking of aromatic rings, the dominant force in asphaltene aggregation.
- **dispersion forces**: van der Waals interactions between alkyl chains.
- **hydrogen bonds**: H-bridges involving heteroatoms (O, N, S).

These interactions directly influence the structure, viscosity, and stability of bitumen. Modern analytical tools are used to visualise and quantify them. From now on, fluently employees:

a) NCI (Non-Covalent Interactions) Analysis:
developed by Johnson et al. (2010), this method relies on the reduced density gradient (RDG) and the sign(λ_2) ρ(r) function to identify and visualise regions of weak interactions. In space, Real 3D. Green isosurfaces indicate π–π interactions, blue ones indicate bridges. hydrogen, and reds the steric repulsions.**[3]**

b) IGMH analysis (Independent Gradient Model Based on Hirschfeld partition):
proposed by Lu et al. (2021), the IGMH uses the Hirschfeld partition of the density molecular real (and not pro-molecular) for separating intra- and inter-fragmentary interactions. This method offers a more rigorous physical basis and isosurfaces that are easier to inspect. visually similar to the original IGM**.[6]**

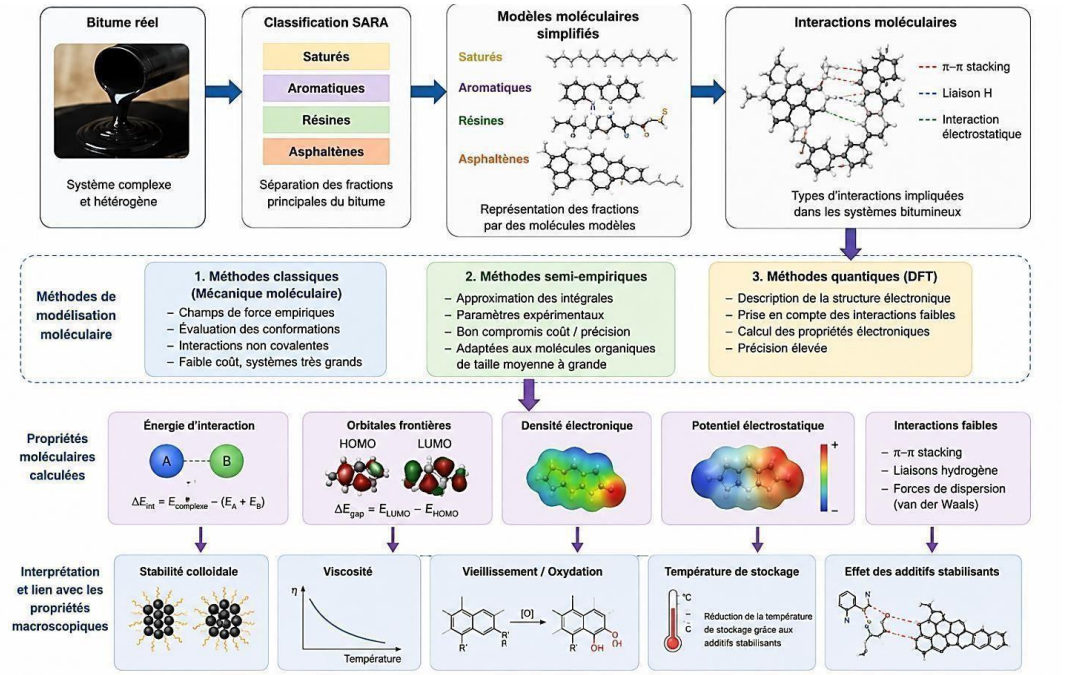


Figure III.2: Schematic representation of weak intermolecular interactions in a bituminous system: (a) π–π stacking between aromatic asphaltene rings, (b) dispersion forces between alkyl chains, (c) hydrogen bonds involving heteroatoms, and (d) visualization by NCI/IGMH analysis of weak interaction isosurfaces (green = π–π, blue = H bridge, red = steric repulsion).

III.5. Recent applications and perspectives

Molecular modelling applied to bituminous systems is experiencing rapid development, driven by increased computing power and improved theoretical methods. Recent application areas include:

Oxidative ageing: Han & Cong (2024) used MD to study the variation in asphaltene aggregation morphology induced by ageing, showing that oxidation increases polarity and

Additives and modifiers: Zhao and al. (2025) used MD to study the effect of nano-ZnO and SBR (Styrene-Butadiene Rubber) on the properties of modified asphalt. **[9]**

Yao and al. (2024) published a review on the prospects for using waste in asphalt via MD, covering recycled materials (rubber, plastic, fibers) and their interactions with the bituminous matrix. **[10]**

Regeneration and bio-additives: the IGM method used Bian and al. (2023) to study the effect of functional group methylation on the disintegration tendency of asphaltenes, paving the way for the development of bio-based regenerators.**[1]**

Conclusion

This chapter outlines the theoretical foundations of molecular modelling in bituminous systems. It discusses the SARA classification for describing bitumen and highlights the Yen-Mullins model, which frames asphaltenes' molecular and colloidal architecture. Molecular modelling techniques employing quantum mechanics and molecular dynamics are emphasised, with a focus on the significance of functional choices for accurate intermolecular interactions. Key theoretical quantities such as interaction energy, HOMO–LUMO gap, and electron density are crucial for understanding stability and reactivity in bituminous systems, with methodological validation against experimental data forming the basis for the subsequent chapters.

References

[1] Lu, T., & Chen, F. (2012). Atomic dipole moment corrected Hirshfeld population method. Journal of Theoretical and Computational Chemistry, 11(01), 163-183.

[2] Gray, M. R., Tykwinski, R. R., Stryker, J. M., & Tan, X. (2011). Supramolecular assembly model for aggregation of petroleum asphaltenes. Energy & Fuels, 25(7), 3125-3134.

[3] Johnson, E. R., Keinan, S., Mori-Sánchez, P., Contreras-García, J., Cohen, A. J., & Yang, W. (2010). Revealing noncovalent interactions. Journal of the American Chemical Society, 132(18), 6498-6506.

[4] Lessa, M. D., Stoyanov, S. R., de Carneiro, J. W. M., & da Costa, L. M. (2024). Density functional theory investigation of the contributions of π-π stacking and hydrogen bonding with water to the supramolecular aggregation interactions of model asphaltene heterocyclic compounds. Journal of Molecular Modeling, 30(5), 145.

[5] Lobato, M. D., Gamez, F., & Pedrosa, J. M. (2021). Evidence of the aggregation behaviour of asphaltenes according to the Yen-Mullins model by direct visualization of their Langmuir-Blodgett films. Fuel, 299, 120872.

[6] Ma, X., Ma, X., Wang, Z., Song, S., & Sheng, Y. (2023). Investigation of changing SARA and fatigue properties of asphalt bitumen under ageing and analysis of their relation based upon the BP neural network. Construction and Building Materials, 394, 132163.

[7] Mullins, O. C., Sabbah, H., Eyssautier, J., Pomerantz, A. E., Barré, L., Andrews, A. B., ... & Zare, R. N. (2012). Advances in asphaltene science and the Yen–Mullins model. Energy & Fuels, 26(7), 3986-4003.

[8] Ravi, S. G., Riazi, M., & Malayeri, M. R. (2025). Determination of averaged representative asphaltene structure through molecular dynamics simulations and analytical methods. Journal of Molecular Liquids, 434, 128043.

[9] Yao, H., Zeng, J., Liu, J., Wang, Y., Li, X., Dai, Q., & You, Z. (2024). Perspectives on the application of waste materials in asphalt based on molecular dynamics simulations: a review. Energy & Fuels, 38(16), 14839-14865.

[10] Xiao, Z., & Chen, T. (2025). Unravelling the molecular mechanism of asphalt binder property: A chemo-structural-mechanical analysis. Construction and Building Materials, 489, 142175.

Chapter IV:

Methodological Section

IV.I. EXPERIMENTAL METHODOLOGY

IV.I.1. Additive synthesis strategy

IV.I.1.1. Choice of precursors and justification

The selection of the four additives is based on a critical analysis of the literature concerning molecular interactions in bituminous systems and their functional complementarity in stabilising bitumen at low temperatures. The precursors were chosen for their commercial availability, moderate cost, and ability to introduce specific functional groups (phenol, amide, ester, long aliphatic chain).

Regarding CIRE (n-octacosane, $C_{28}H_{58}$), its selection is based on three criteria:

- Its melting point of 61–63°C is consistent with the summer service temperatures of Algerian pavements (up to ~60°C), allowing reversible crystallisation/decrystallization in service. **[1]**
- The C28 chain length is documented as optimal for the plasticising effect of modifying the paraffin-bitumen phase transition in Algerian paraffinic bitumens. **[2]**
- A commercial purity of ≥ 98% is sufficient for the planned rheological tests.

The absence of synthetic materials is assumed and justified by these criteria.

Table IV.I.1: Precursors and target functional groups

Additive	Main precursor	Target functionalgrouping	Intended role
PHEN	Phenol + tert-butanol (excess 2.5 eq.)	Phenolic hydroxyl+ tert-butyl	Antioxidant (ROO• radical scavenger)
BENZ	Benzoyl chloride + aniline	Secondaryamide (N–H, C=O)	Colloidal polarity and cohesion modifier
PLAS	Benzoic acid + Benzoyl alcohol	Aromatic ester (C=O, C–O–C)	Plasticiser (reduction of Tgby van der Waals interactions)
WAX	n-Octacosane ($C_{28}H_{58}$) commercial ≥ 98%	C_{28} linear aliphatic chain	Transition temperature reducer (crystallisation/decrystallization)

IV.I.1.2. Selection of reactions

The synthetic routes were chosen according to the criteria of yield, selectivity and ease of implementation. For PHEN, a tert-butanol/phenol ratio of 2.5 equivalents is used in order to shift the equilibrium towards ortho disubstitution and to optimise the yield.

Table IV.I.2: Selection of reactions and justifications

Additive	Reaction	Justification
PHEN	Friedel-Crafts alkylation	Selective introduction of two tert-butyl groups ortho to the phenolic OH; ratio 1:2.5 to promote dialkylation;yield 65–75%
BENZ	Acylation (acyl chloride)	Formation of a secondary amide with a high yield (85%); temperature control to limit side reactions
PLAS	Fischer esterification	Equilibrium shift by water trapping (4Å molecular sieves); excellent efficiency (90%)
CIRE	—	Commercial product of high purity (≥ 98%); purity validated as sufficient for the intended rheological tests.

IV.I.2. Experimental synthesis protocols

IV.I.2.1. Synthesis of 2,6-di-tert-butylphenol (PHEN)

a) Reaction principle

Friedel-Crafts alkylation of phenol by tert-butanol (2.5 eq.), catalysed by dilute sulfuric acid (5%), leads to selective substitution at ortho positions (2 and 6) of the aromatic ring (Figure IV.I.1):

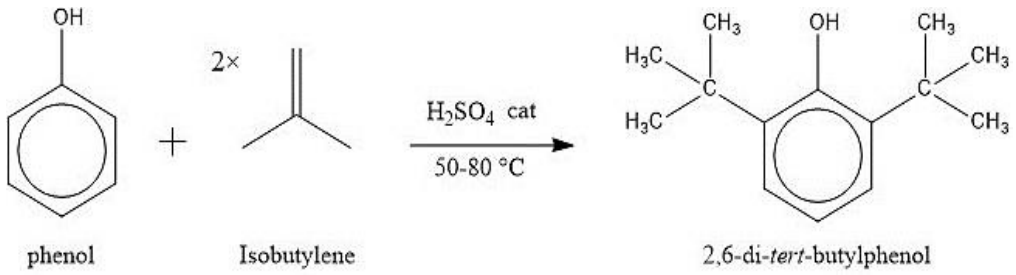


Figure IV.I.1: Reaction scheme for the synthesis of 2,6-di-tert-butylphenol (PHEN).

a) Reagents and quantities

Table IV.I.3: Reagents for the synthesis of PHEN

Reagent	Quantity	n (mol)	Role
Phenol	9.4 g	0.10	Aromatic substrate
tert-Butanol	18.5 g	0.25	Alkylating agent (excess 2.5 eq.)
H_2SO_4 5% (aq.)	50 mL	—	Acid catalyst
Toluene	100 mL	—	Extraction solvent
NaOH 10% (aq.)	50 mL	—	Neutralization
Hexane	30 mL	—	Recrystallization

C) Detailed operating procedure

1. Catalyst preparation: Under a fume hood, dilute 5 mL of concentrated H_2SO_4 in 95 mL of ice water. Cool to 20°C before use.

2. Alkylation reaction: Introduce 9.4 g of phenol into a 250 mL round-bottom flask with 50 mL of 5% H_2SO_4. Heat to 85–90°C under reflux. Add 18.5 g of tert-butanol dropwise over 2 h. Maintain reflux for an additional 6 h. Monitor by TLC (eluent: hexane/AcOEt 9:1).

3. post-reaction treatment (2 h): Cool to 25°C. Neutralise with 10% NaOH to pH 7–8. Extract 3 times with 30 mL of toluene. Wash with water (2 × 50 mL), dry over anhydrous Na_2SO_4, filter, and evaporate.

4. Purification: Recrystallise in 30 mL of hot hexane; cool to 4°C; filter. Product: white solid, Pf = 35–37°C. Yield: 65–75%.

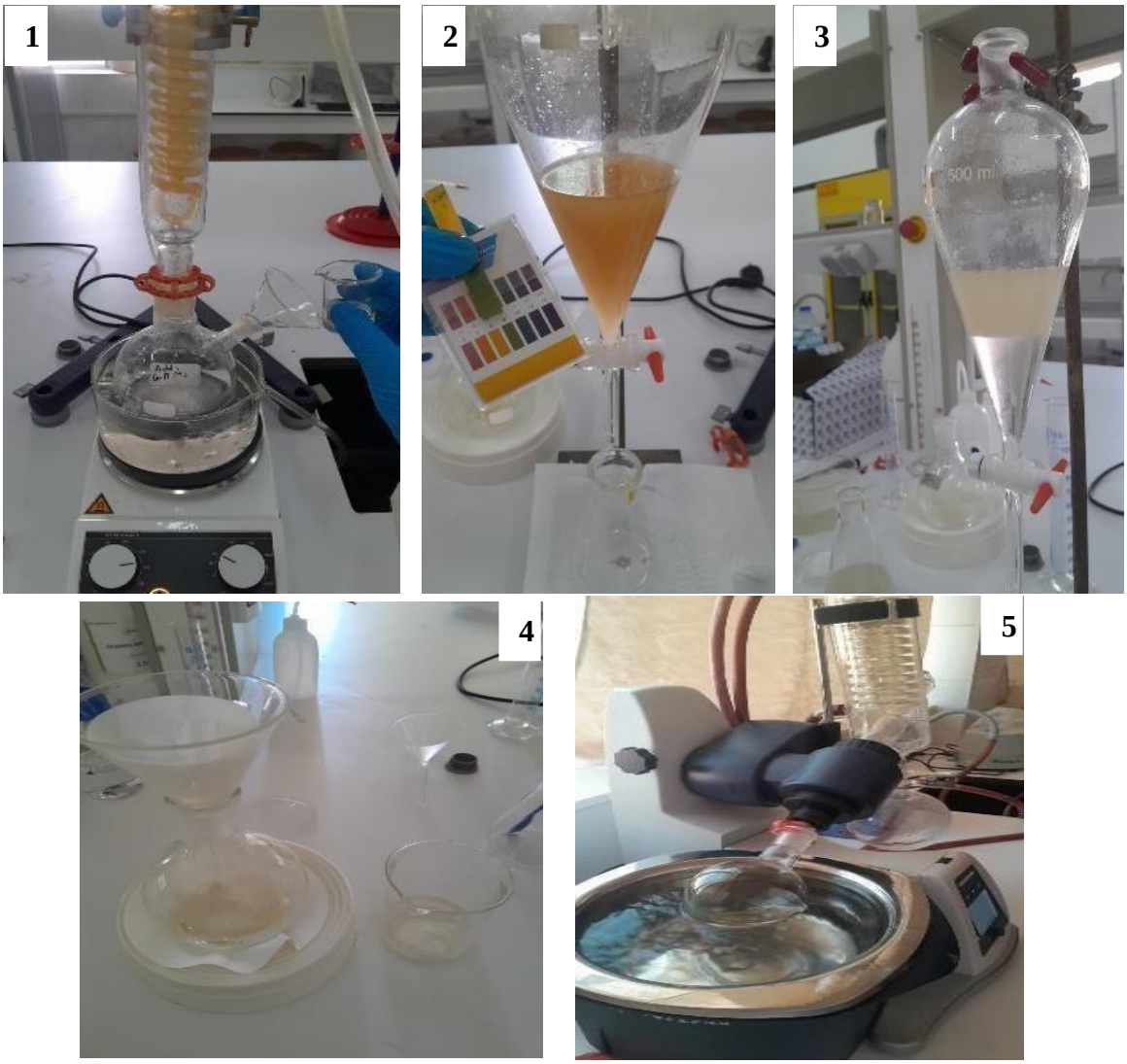


Figure IV.I.2: Experimental setup for the synthesis of PHEN (**1**: reflux heating setu, **2**: Neutralisation with NAOH, **3**: phase separation, **4**: dry over anhydrous Na_2SO_4, filter), **5**: and evaporate.



Figure IV.I.3: PHEN product obtained.

IV.I.2.2. Synthesis of N-phenylbenzamide (BENZ)

a) Reaction principle

Acylation of aniline by benzoyl chloride in the presence of anhydrous triethylamine (HCl trap base) in DCM (Figure IV.I.2):

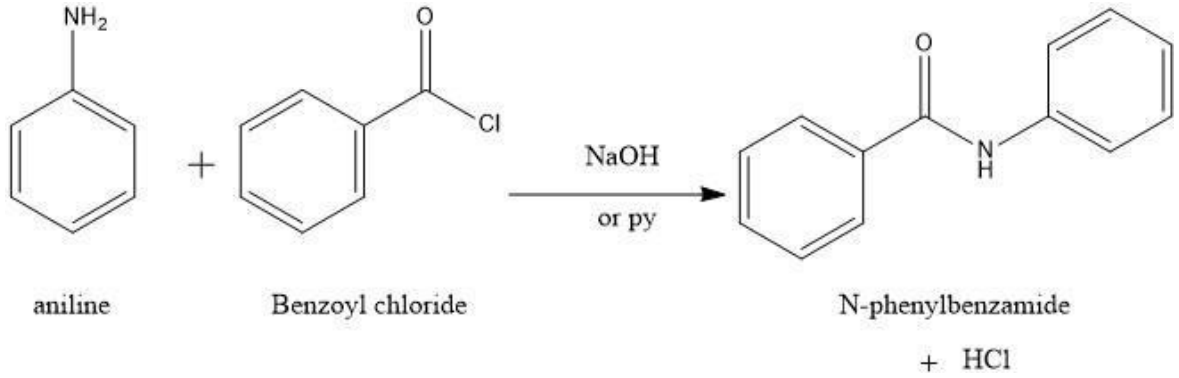


Figure IV.I.4: Reaction scheme for the synthesis of N-phenylbenzamide (BENZ) by acylation of aniline.

a) Reagents and quantities

Table IV.I.4: Reagents for the synthesis of BENZ

Reagent	Quantity	n (mol)	Role
Benzoyl chloride	14.1 g	0.10	Acylating agent
Aniline	9.3 g	0.10	Amino nucleophile
Triethylamine	8.0 mL (6.3 g)	0.10	HCl trap base
Dichloromethane (DCM)	50 mL	—	Reaction solvent
$NaHCO_3$ 5% (aq.)	100 mL	—	Washing
Ethanol	40 mL	—	Recrystallization

b) Detailed operating procedure:

1. Preparation of the base (15 min): Pipette 8.0 mL of Triethylamine and store in a sealed bottle under an inert atmosphere at 20°C.
2. Acylation reaction: Dissolve 14.1 g of benzoyl chloride in 50 mL of DCM and place in an ice bath (0°C). Add Triethylamine dropwise over 15 min.

Introduce 9.3 g of aniline dropwise over 30 min (T < 25°C). Stir for 30 min, then heat at 40°C for 1 h. Verify by TLC (Rf ≈ 0.6, hex/AcOEt 8:2).

3. Purification: Wash 3 times with water (3 × 50 mL), then with 5% $NaHCO_3$ (2 × 50 mL), then with water (50 mL). Dry over Na_2SO_4, filter, and evaporate. Recrystallise in 40 mL of hot ethanol (70°C); cool to 4°C; filter. Product: white solid, Pf = 163°C. Yield: 85%.



Figure IV.I.5: Photograph of the experimental setup for the synthesis of BENZ

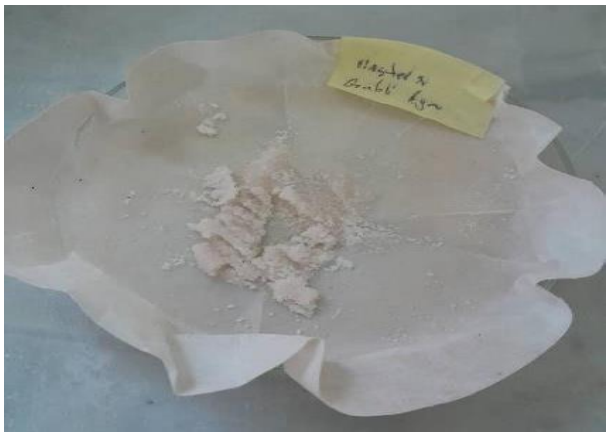


Figure IV.I.6*:* Product BENZ (N-phenylbenzamide) recrystallised in ethanol.

IV.I.2.3. Synthesis of benzyl benzoate (PLAS)

a) Reaction principle

Fischer esterification of benzoic acid with benzoyl alcohol

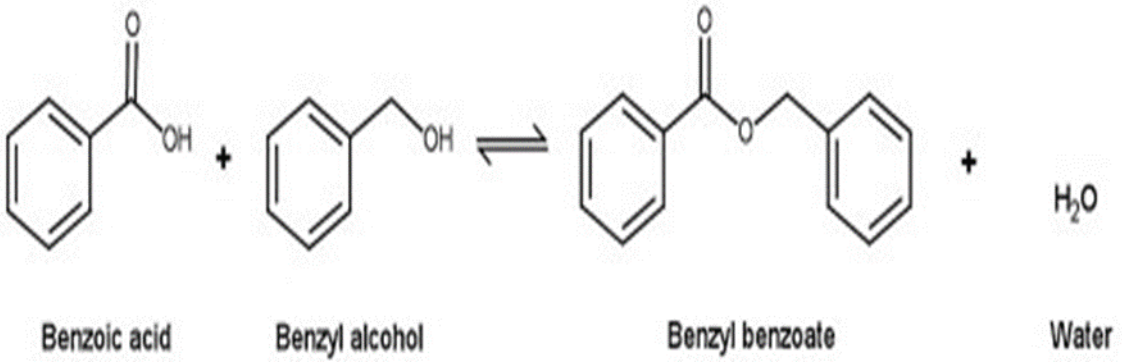


Figure IV.I.7: Reaction scheme for the synthesis of benzyl benzoate (PLAS) by Fischer esterification.**[11]**

Table IV.I.5: Reagents for PLAS synthesis

Reagent	Quantity	n (mol)	Role
Benzoic acid	36.6 g	0.10	Carboxylic acid
Benzyalcohol	38.1 g	0.10	Alkylating agent
H_2SO_4 conc. (cat.)	1.5 mL	Catalyst	Acid catalyst
Dry toluene	300 mL	—	Solvent azeotropic trainer
Anhydrous Na_2CO_3	31.8g (0.1 mol)	Capture HCl(REPLACES pyridine)	Anhydrous Na_2CO_3
anhydrous $MgSO_4$	45 g	Dehydrating (if not Dean-Stark)	anhydrous $MgSO_4$

C) Detailed operating procedure

1. Esterification: Place the sieves, 36.6 g of benzoic acid, 38.1g of benzyl chloride, and 300 mL of dry toluene in the flask. Add 1.5 mL of concentrated H_2SO_4 dropwise add 45g Mgso4. Heat under reflux (110°C) for 6.5 h. Monitor by TLC (Rf ≈ 0.8, hexane/AcOEt 9:1). Filter through the sieves.
2. Purification: Wash with distilled water 2×100 mL (remove residual salts) Wash with 3×30 mL of diluted 1% HCl (if the phase is cloudy, remove carbonates). Wash with water 2×100 mL → clear organic phase
3. Dry over Na_2SO_4, filter, and evaporate. Purify by short vacuum distillation (195°C / 15 mmHg). Product: colorless oil, nD = 1.567. Yield: 90%.



Figure IV.I.8: PLAS synthesis setup

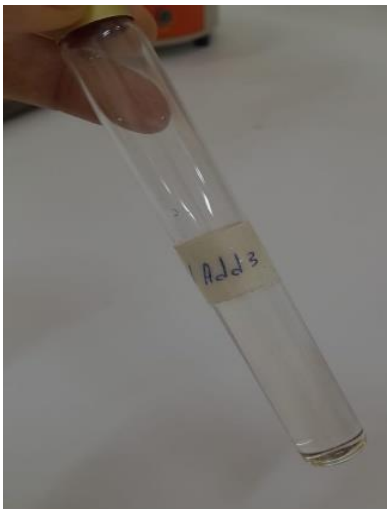


Figure IV.I.9: PLAS (benzyl benzoate) product after distillation under

IV.I.2.4. Commercial additive: n-Octacosane (CIRE)

n-Octacosane ($C_{28}H_{58}$, purity≥ 98%) is used as is, without prior treatment. The justification for this lack of purification is explained in §4.1.1 **[1]**. Pf = 61–63°C.

IV.I.3. Experimental characterisation of additives

IV.I.3.1. Analytical techniques used

All four additives were characterised by IR spectroscopy (FTIR, KBr pellet or film) and by measuring the melting point or refractive index for liquids. TLC also monitored the three synthesised additives (PHEN, BENZ, PLAS). ^{1}H NMR ($CDCl_3$, 300 MHz) was acquired for PHEN and CIRE (confirming the structure), and for BENZ and PLAS (results shown below, Figures 4.5–4.8). ^{13}C NMR, planned in the initial study, could not be performed due to time constraints and lack of access to the instrument.

IV.I.3.2. Characterisation Data

Table IV.I.6: Spectroscopic and Physicochemical Characterisation of the Synthesised Additives (PHEN, BENZ, PLAS, and CIRE)

Additive	IR (cm^{-1})	^{1}H NMR (ppm)	Pf / other
PHEN	3600 (free OH); 1500–1600 (C=C arom.)	δ 1.3 (18H, tBu); 4.7 (1H, OH); 7.1–7.3 (3H, flavor)	Mp = 35–37°C; TLC Rf = 0.4
BENZ	3300 (N–H); 1650 (C=O amide); 1595 (C=C arom.); 694 (C–H mono-subst.)	δ 7.1 (1H, N–H, s); 7.3–7.5 (5H, Ph-CO); 7.5–7.7 (5H, Ph-NH)	Pf = 163°C; CTM Rf = 0.6
PLATES	1720 (C=O ester); absence of OH band at 3400; 1270 (C–O–C); 750 (C–H aroma)	δ 5.2 (2H, OCH_2, s); 7.3–8.1 (10H, 2 × Ph)	Liquid; nD = 1.567; TLC Rf = 0.8
CIRE	2920, 2850 (C–H aliph.); 720 (balancement CH_2)	δ 0,88 (t, CH_3); 1,25 (m, $(CH_2)_{26}$)	Pf = 61–63°C; produit commercial ≥ 98%

IV.II. MOLECULAR MODELING METHODOLOGY

IV.II.1. Selection of model molecules

IV.II.1.1. Additives studied

Table IV.II.1: Modelled additives and expected mechanisms of action

No.	Additive	Formula	Main function	Symbol
A1	2,6-di-tert-butylphenol	$C_{14}H_{22}O$	Antioxidant (free radical scavenger)	PHEN
A2	N-phenyl benzamide	$C_{13}H_{11}NO$	Polarity modifier	BENZ
A3	Benzyl benzoate	$C_{14}H_{12}O_2$	Plasticizer	PLATES
A4	n-Octacosane	$C_{28}H_{58}$	Réducteur de température de transition	CIRE

IV.II.1.2. Representative molecular models of SARA fractions

In accordance with the SARA approach, each fraction is represented by a unique model compound.

The simplifications adopted are explicitly assumed.

Table IV.II.2: SARA molecular models; rationale and limitations

SARA Fraction	Model compound	Formula	Symbol	Justification and limitations
Saturates	Squalene	$C_{30}H_{62}$	SQUA	Branched alkane; continuous fluid phase. Validated by Greenfield (2011)
Aromatics	Corona	$C_{24}H_{12}$	CORO	Condensed aromatic polycycle; site of π-π interactions. Limitation: simplification of real thiophene structures.
Resins	Benzoic acid	$C_7H_6O_2$	ACID	Represents carboxylic acid functions. Limitation: underestimation of the dispersion contribution (actual molar mass 500–1500 g/mol).

Asphaltenes	Porphyrin Ni (II)	$C_{20}H_{14}N_4Ni$	PORP	Metallic aromatic heterocycle. Limitation: ignores peripheral alkyl chains.

IV.II.2. Computational Environment and Software

Table IV.II.3: Software used

Software	Version	Role in the study
Gaussian 16	Rev. C.01 **[5]**	DFT calculations: optimisation, frequencies, interaction energies
Multiwfn	3.8 **[6]**	QTAIM analysis, NBO, NCI visualisation
VMD	1.9.4 **[7]**	3D rendering of structures
Material Studio	2021 (BIOVIA) **[8]**	Construction of bitumen-additive complexes and preparation of systems
Discovery studio visualizer	2021 **[9]**	Analysis and graphical visualisation of molecular results

IV.II.3. DFT Calculation Parameters

IV.II.3.1. Choice of the functional

The ωB97X-D functional (range-separated hybrid with integrated D2 dispersion correction, Chai and Head-Gordon, 2008) **[3]** was chosen for the following reasons:

- Range separation: correct handling of long-range interactions (π-π, H-bond)
- D2 dispersion correction: essential for non-covalent interactions (van der Waals, CH···π)
- Accuracy: error ~0.25 kcal/mol on HB23 benchmark.**[16]**
- Bibliographic validation: established use for bituminous systems.

IV.II.3.2. Calculation parameters

Table IV.II.4: DFT Parameters

Setting	Value	Justification
Functional	ωB97X-D	Hybrid with range separation + dispersion D2 **[3,10]**
Base	6-311++G(d,p)	Double zeta + diffuse + polarisation ; standard for non-covalent interactions
Implicit solvent	SMD / Toluene (ε = 2.379)	Nonpolar environment of bitumen; validated by PCM **[4]**

Formula for interaction energy:

$$\mathbf{\Delta E}_{int} = \boldsymbol{E}_{complex} - (\mathbf{E}_{additive} + \mathbf{E}_{compound\ SARA})$$

IV.II.3.3. Solvation Model

The SMD model (Marenich et al., 2009) **[4]** is applied to toluene (ε = 2.379). The PCM model **(ε = 2.5)** is used for validation.

IV.II.4. Calculation Protocols

IV.II.4.1. Geometric optimisation of monomers

1. The first phase consists of optimising the eight pure monomers (4 additives + 4 SARA): Download advertising material
2. DFT optimization: ωB97X-D/6-311++G(d,p),
3. Validation: All positive frequencies (true minimum);
4. The optimised geometries are shown in Figures 5.1 and 5.2.

IV.II.4.2. Post-calculation analyses

Table IV.II.5: post-calculation analysis methods

Method	Description	Software	Extracted information
QTAIM [8]	Critical connection points (CCPs)	Multiwfn **[6]**	Topology of interactions
NCI (RDG)	Reduced densitygradient isosurfaces	Multiwfn **[6]** + VMD **[7]**	Spatial mapping of interactions

REFERENCES

[1] Tarrer, A. R., & Wagh, V. P. (1992). Innovative tests to predict the strength and type of asphalt-aggregate bonds. Fuel science & technology international, 10(4-6), 457-474.

[2] Lemesre, L., Frances, F., Grandjean, A., & Gossard, A. (2019). Hybrid colloidal suspensions tailored as gels to remove radioactive bitumen stains. Journal of environmental management, 232, 660-665.

[3] Chai, J. D., & Head-Gordon, M. (2008). Long-range corrected hybrid density functionals with damped atom–atom dispersion corrections. Physical Chemistry Chemical Physics, 10(44), 6615-6620.

[4] Marenich, A. V., Cramer, C. J., & Truhlar, D. G. (2013). Generalized born solvation model SM12. Journal of Chemical Theory and Computation, 9(1), 609-620.

[5] Frisch, M. E., Trucks, G. W., Schlegel, H. B., Scuseria, G. E., Robb, M., Cheeseman, J. R., ... & Fox, D. J. (2016). Gaussian 16.

[6] Lu, T., & Chen, F. (2012). Multiwfn: A multifunctional wavefunction analyzer. Journal of computational chemistry, 33(5), 580-592.

[7] Humphrey, W., Dalke, A., & Schulten, K. (1996). VMD: visual molecular dynamics. Journal of molecular graphics, 14(1), 33-38.

[8] Meunier, M., & Robertson, S. (2021). Materials studio 20th anniversary. Molecular Simulation, 47(7), 537-539.

[9] Systèmes, D. (2021). BIOVIA Discovery Studio Visualizer (Version 21.1. 0.20298)[Software].

[10] Mann, E. L., Wagen, C. C., Vandezande, J. E., Wagen, A. M., & Schneider, S. C. (2025). Egret-1: Pretrained neural network potentials for efficient and accurate bioorganic simulation. arXiv preprint arXiv:2504.20955.

[11] https://www.sciencedirect.com/science/article/pii/S1359511319313911

Chapter V:

Results And Discussion

V.I. Experimental Results

V.I.1. Synthesis and characterisation results of additives

V.I.1.1 Yields and appearance of the products obtained

The additives PHEN (A_1), BENZ (A_2), and PLAS (A_3) were synthesised in the laboratory according to the protocols described in Chapter IV, while the additive CIRE (A_4), n- octacosane ($C_{28}H_{58}$), is a commercial product of purity ≥ 98% used without prior purification. The measured yields, physical appearance, and melting points are summarised in Table V.1.

Table V.I.1: Physical characterisation and yields of additives synthesised in the laboratory

Additive	Reaction	Yield (%)	Appearance	Measured temperature (°C)	Tf literature (°C) [ref.]
A_1	Friedel-Crafts alkylation	70-85	Solid white	35-37	35-37
A_2	Acylation	75-90	Yellow powder	163	162-164
A_3	Fischer esterification	80-95	Colorless crystals	_____	_____
A_4	Commercial (n-octacosane ≥ 98%)	____	Solid white waxy	61-63	61-64

V.I.1.2. Characterisation by UV-visible spectroscopy

The UV-visible spectra of the four additives were recorded in absolute ethanol at a concentration of 10^{-4} mol·L^{-1}, between 200 and 400 nm. The wavelengths of maximum absorption (λ_max) and the assignments of the electronic transitions are summarised in Table VI2, and the spectra are shown in Figure VI1.

PHEN exhibits an absorption band at λmax = 266 nm attributed to the π→π* transition of the substituted phenolic ring, and a shoulder at [value] nm corresponding to the n→π* transition of the hydroxyl group.

BENZ shows more intense absorption due to the extended conjugation between the amide carbonyl and the two phenyl rings. PLAS displays a similar profile characteristic of conjugated aromatic esters.

CIRE, lacking any π chromophore, shows no significant absorption beyond 250 nm, confirming the purely aliphatic nature of its structure.

Table V.I.2: UV-visible data for the four additives (EtOH, 10^{-4} mol·L^{-1})

Additive	**λ_max (nm)**	**ε (L·mol⁻¹·cm⁻¹)**	**Attribution**	**Chromophore**
(A_1)	to be completed	to be completed	π→π* (phenolic nucleus)	C=C arom.
(A_2)	to be completed	to be completed	π→π* (conjugated amide)	C=O, C=C
(A_3)	to be completed	to be completed	π→π* (aromatic ester)	C=O, C=C
(A_4)	absence of band > 250 nm	—	No aromatic chromophores	Aliphatic chain

V.I.1.3. Structural confirmation by comparison with the literature

During the synthesis period, access to IR and NMR spectrometers was not possible. Structural confirmation, therefore, relies on two complementary elements: (i) the agreement of the measured melting points with values reported in the literature for the same compounds, and (ii) the consistency of the recorded UV-visible spectra with the expected chromophores for each structure.

For reference, Table V.I.3 presents IR and ^{1}H NMR spectroscopic data from the literature for the four additives. These data, not measured in this work, are provided to allow for future complete identification of the products obtained and to guide the interpretation of spectra acquired during the continuation of this work.

The agreement between the measured melting points and the values in the literature (Table V.I.1), combined with the consistency of the UV-visible spectra, provides a body of concordant evidence supporting the identity of the products obtained. Acquisition of IR and ^{1}H NMR spectra is planned as the immediate next step in this work to provide complete structural confirmation.

Table V.I.3: Reference spectroscopic data (literature) for the four additives

Additive	Characteristic IR bands (cm^{-1})	Characteristic ^1H NMR signals (ppm)	Ref.
PHEN (A_1)	3600 (O–H free); 1500–1600 (C=C arom .); 1230 (C–W)	δ 1.3 (s, 18H, 2×C (CH_3) $_3$);4.7(s,1H, OH); 7.1–7.3 (m, 3H, arom.)	NIST Chemistry WebBook
BENZ (A_2)	3300 (N–H); 1650 (C=O amide); 1595 (C=C arom.)	δ 7.1 (s, 1H, N–H); 7.3–7.7 (m, 10H, 2×Ph)	SDBS Spectral Database
PLAS (A_3)	1720 (C=O ester); 1270 (C–O–C); absence O–H	δ 5.2 (s, 2H, OCH_2); 7.3–8.1(m,10H, 2×Ph)	SpectraBase
WAX (A_4)	2920, 2850 (C–H aliph.); 720 (CH_2 balance)	δ 0.88 (t, 3H, CH_3); 1.25 (m,52H, (CH_2) $_{2\ 6}$)	NIST Chemistry WebBook

V.II. Molecular modelling results

V.II.1. Geometric optimisation of additives and bitumen models

All the molecular structures studied—the four additives (PHEN/A_1, BENZ/A_2, PLAS/A_3, CIRE/A_4) and the four SARA model molecules (SQUA, CORO, ACID, PORP) were optimised at the ωB97X-D/6-311++G (d, p) theory level using Gaussian 09 software. The absence of imaginary frequencies was verified for all structures, confirming that the obtained geometries correspond to real minima on the potential energy surface. Figures V.II.1 and V.II.2 show the optimised structures of the four additives and the SARA models, respectively.

Analysis of the optimised geometries reveals characteristic conformations directly related to the chemical nature of each additive.

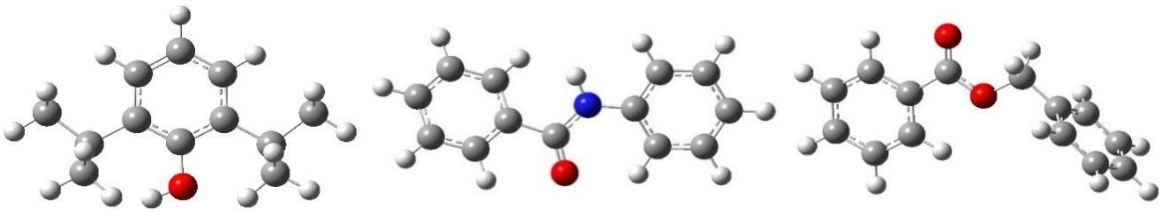
PHEN (A_1): Despite the presence of two tert -butyl groups in ortho positions, PHEN (A_1) adopts a planar conformation with an O–C–C–C dihedral angle of 180°, indicating that the hydroxyl group remains in the plane of the aromatic ring.

This coplanarity maximises the conjugation between the oxygen's lone pair and the aromatic π system, enhancing **PHEN's** electron-donating character and its ability to stabilise free radicals by transferring hydrogen to oxidised asphaltenes.

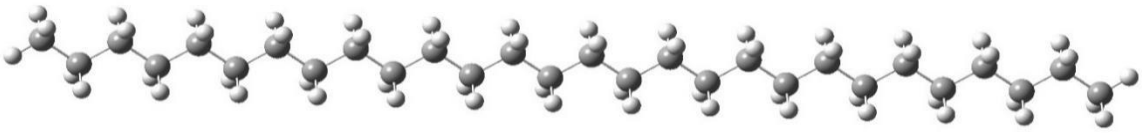
BENZ (A_2): exhibits a quasi-planar geometry (dihedral angle = 43.22°), favouring extensive conjugation between the carbonyl of the amide and the two phenyl rings, conducive to π–π interactions with the polycyclic systems of asphaltenes.

PLAS (A_3): shows a planar conformation (dihedral angle = 180°) around the C (=O) –O bond, favouring maximum conjugation between the carbonyl and the aromatic ring, characteristic of conjugated aromatic esters.

CIRE (A_4): adopts an all- trans conformation (planar zigzag), minimising steric repulsions between the 26 methylene groups, in agreement with the crystallographic data of n- octacosane.



2,6-di-tert-butylphenol (A_1) N-phenylbenzamide (A2) Benzyl benzoate (A3)

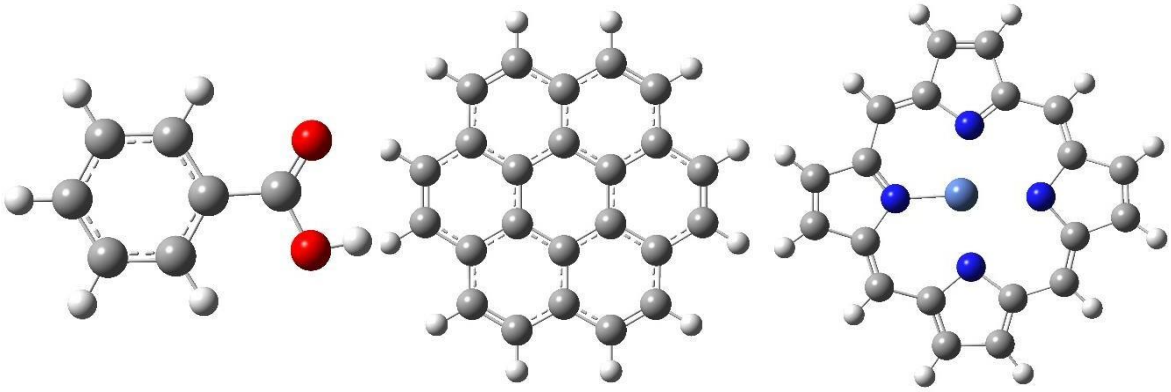


n-Octacosane

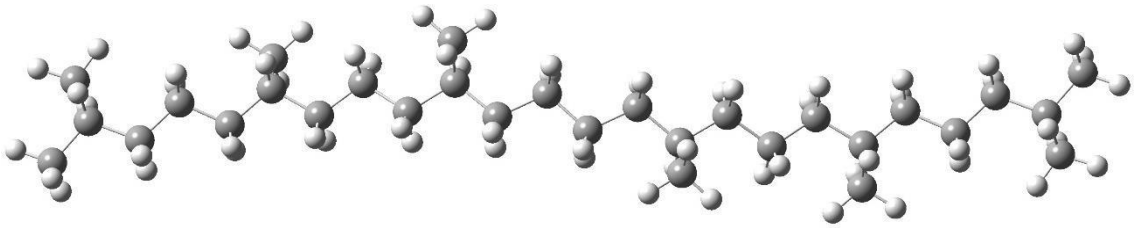
Figure V.II.1: Optimised structures of additives (PHEN, BENZ, PLAS, CIRE) obtained atthe theoretical level wB97X-D/6-311++G (d,p)

Table V.II.1: Main geometric parameters of the four additives optimised at the WB97X-D/6-311++G (d, p) level.

Setting	PHEN (A_1)	BENZ (A_2)	PLAS (A_3)	WAX (A_4)
d(C–O) phenol/ester (Å)	1,362	—	1,342	—
d(C=O) amide/ester (Å)	—	1,220	1,211	—
d(C–N) amide (Å)	—	1,372	—	—
d(C–C) chain (Å)	—	—	—	1,527
θ(C–O–H) phenol (°)	109.5	—	—	—
θ(C–C=O) (°)	—	121.3	124.4	—
Plane dihedral angle. (°)	180	43.22	180	—



Benzoic acid Corona Ni-Porphyrin



Squalane

Figure V.II.2: Optimised structures of the SARA models (ACID, CORO, PORP, SQUA) obtained at the theory level wB97X-D/6-311++G (d,p).

V.II.2. Electronic properties of additives

The energies of the HOMO and LUMO frontier orbitals, the energy gap $\Delta EHOMO-LUMO$, and Parr global reactivity descriptors are presented in Table V.II.2 and Table V.II.3.

The HOMO–LUMO gap is an indicator of overall chemical reactivity: a small gap reflects high polarizability and a greater capacity for charge-transfer interactions. The additives are ranked according to their increasing gap as follows: BENZ (8.63 eV) < PLAS (9.64 eV) < PHEN (9.85 eV) < CIRE (14.21 eV). BENZ (A_2) has the smallest gap (8.63 eV), confirming its increased reactivity and its ability to interact with the polar fractions of asphaltenes via donor-acceptor interactions. PHEN (A_1), with moderate electrophilicity (ω = 0.793 eV) and a HOMO localised on the phenolic ring, confirms its electron-donating character, consistent with its role as a radical antioxidant. CIRE (A_4), with the highest band gap (14.21 eV) and maximum hardness (η = 7.10 eV), exhibits a chemically inert character acting exclusively through van der Waals interactions, consistent with its role as a fluxing agent.

Table V.II.2: Energy parameters and overall reactivity descriptors of the additives studied.

Descriptor	PHEN (A_1)	BENZ (A_2)	PLAS (A_3)	WAX (A_4)
E (kcal/mol)	-390197.56	-396,465.56	-433,588.29	-691,361.79
E^{HOMO} (eV)	-7.72	-7.94	-8.90	-9.64
E^{LUMO} (eV)	2.13	+0.69	+0.74	+4.57
L–H gap (eV)	9.85	8.63	9.64	14.21
Dipole moment μ (D)	1.96	3.44	2.27	0
Chemical potential μ (eV)	-2.795	-3.62	-4.08	-2.53
Hardness η (eV)	4.925	4.31	4.82	7.10
Softness σ (eV^{-1})	0.203	0.23	0.20	0.14
Electronegativity χ (eV)	2.795	3.62	4.08	2.53
Electrophilicity ω (eV)	0.793	1.52	1.72	0.45

Regarding the SARA models (Table V.II.3), squalane (SQUA) exhibits the highest band gap (13.98 eV) and the maximum hardness (η = 6.990 eV), confirming its chemically inert character, representative of saturated compounds. Ni-porphyrin (PORP) exhibits the lowest band gap (5.13 eV) and the highest softness (σ = 0.3899 eV^{-1}), making it the most reactive and polarizable;

This result is consistent with the presence of the central metal Ni (II). This high reactivity of PORP explains its high affinity for the functional additives observed in the interaction calculations. Coronene (CORO) and benzoic acid (ACID) exhibit intermediate values.

Figure V.II.3 illustrates the spatial distribution of the HOMO and LUMO frontier orbitals of the four additives. The HOMO of PHEN (A_1) is localised on the aromatic ring and the oxygen atom, confirming its electron-donating character. The HOMO of BENZ (A_2) is delocalized over the entire conjugated π-amide-phenyl system, consistent with its smallest band gap (8.63 eV). The HOMO of PLAS (A_3) is concentrated on the aromatic ester group, indicating preferential sites for interaction with electrophilic fractions. CIRE (A_4) exhibits highly diffuse orbitals on the alkyl chain, in agreement with its chemically inert character (band gap = 14.21 eV).

Table V.II.3: Overall reactivity descriptors of SARA model molecules.

Descriptor	Benzoic acid ACID	Corona CORO	Porphyri Ni (II) PORP	Squalane SQUA
E (kcal/mol)	-263990.43	-578312.66	-1566321.70	-740693.17
E^{HOMO} (eV)	-9.15	-7.20	-6.36	-9.55
E^{LUMO} (eV)	0.60	0.16	-1.23	4.43
L–H gap (eV)	9.75	7.36	5.13	13.98
Dipole moment μ (D)	1.90	0	3.98	0.002
Chemical potential μ (eV)	-4.275	-3.520	-3.795	-2.560
Hardness η (eV)	4.875	3,680	2,565	6,990
Softness σ (eV^{-1})	0.2051	0.2717	0.3899	0.1430
Electronegativity χ (eV)	4,275	3,520	3.795	2,560
Electrophilicity ω (eV)	1,874	1.684	2,808	0.469

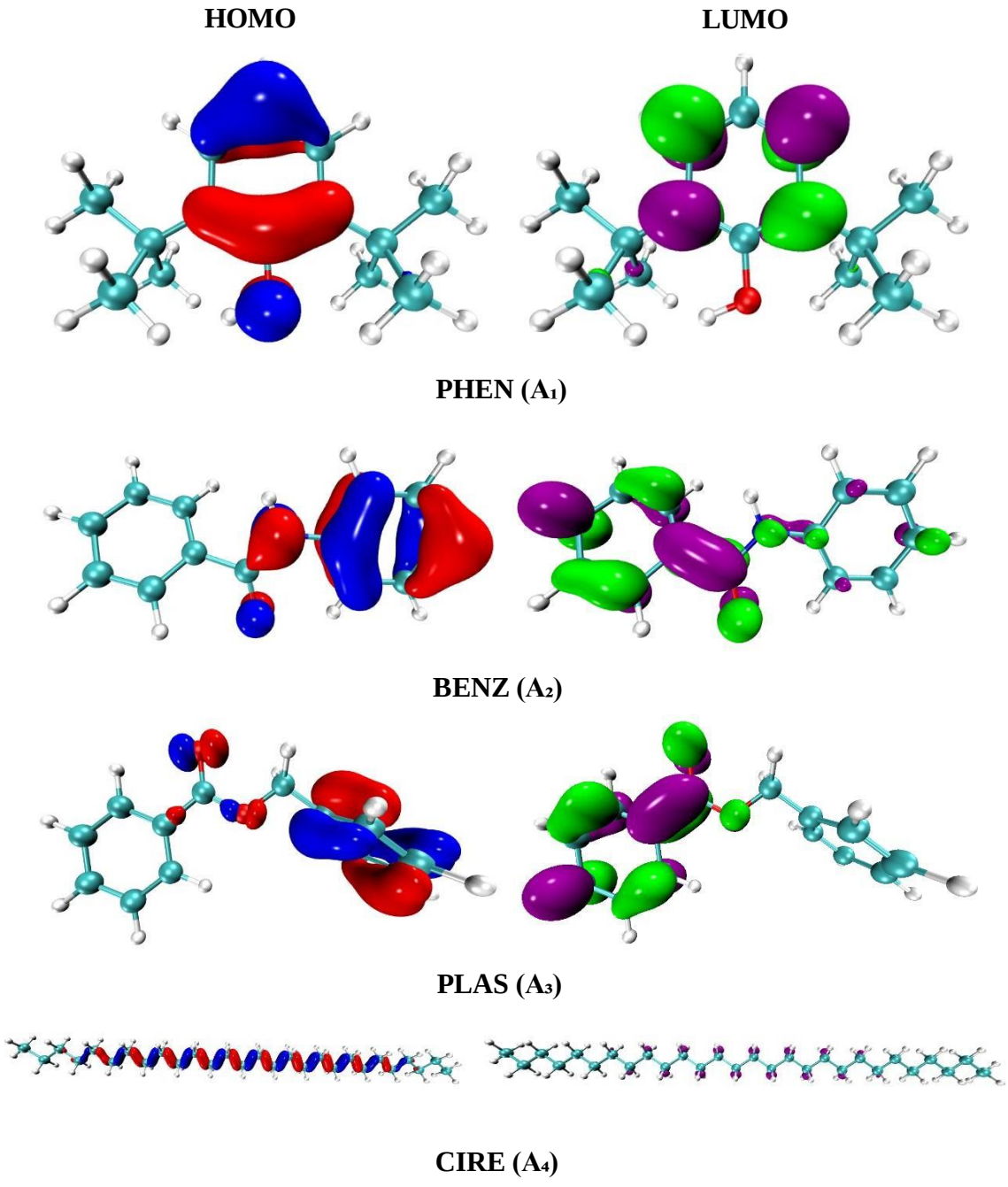


Figure V.II.3: Representation of the HOMO and LUMO frontier orbitals of the additives PHEN (A_1), BENZ (A_2), PLAS (A_3), and CIRE (A_4) calculated at the theoretical ωB97X-D /6-311++G (d, p) level.

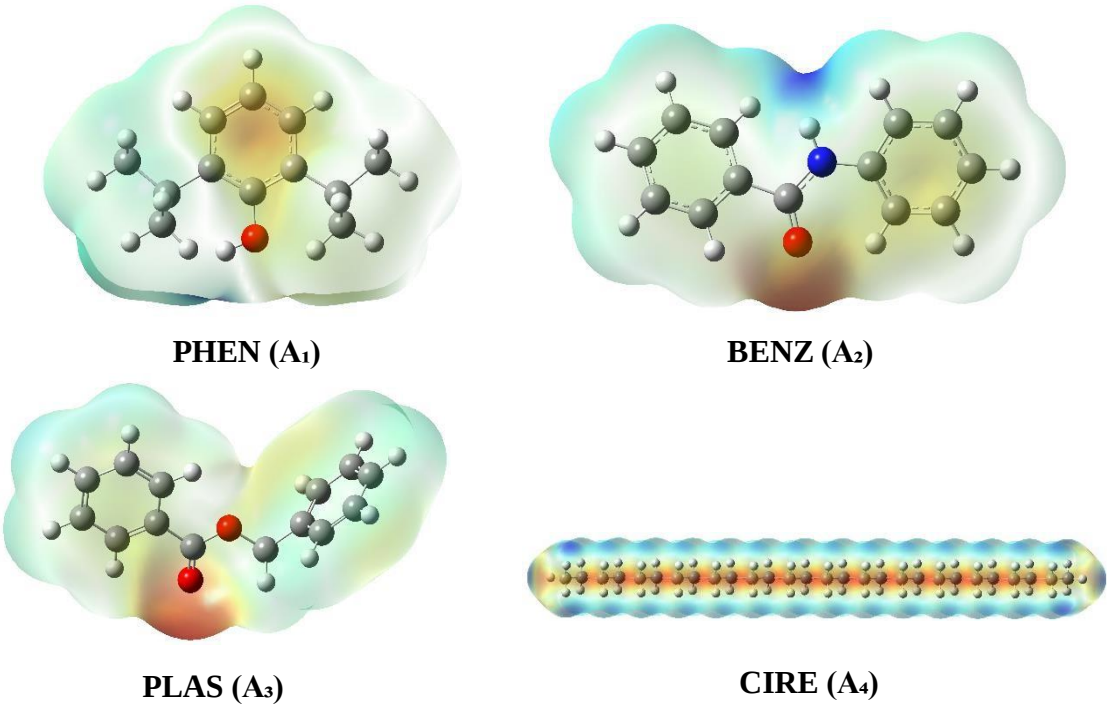


Figure V.II.4: ESP maps of the four studied additives at the ωB97X-D/6-311++G (d, p) level (iso = 0.004 a.u.) (red: nucleophilic region; blue: electrophilic **region)**

The electrostatic potential maps (Figure V.II.4) reveal distinct preferential interaction sites for each additive. PHEN (A_1) exhibits a nucleophilic region (red) concentrated on the oxygen of the hydroxyl group, confirming its hydrogen bond donor character. BENZ (A_2) shows high electron density on the nitrogen and oxygen of the amide group, consistent with its ability to form hydrogen bonds with the heteroatoms of asphaltenes. PLAS (A_3) presents a red region on both ester oxygens, which are the preferential interaction sites with polar fractions. CIRE (A_4), on the other hand, displays a nearly uniform green/yellow surface, confirming the absence of any marked reactive site and its non-polar character.

V.II.3. Additive interaction energies–SARA

The interaction energies of the 16 additive binary-SARA complexes were calculated using the Adsorption Locator method of the Forcite module in Material Studio, with the COMPASS III force field.

For each complex, several orientation configurations were generated, and the most stable configuration, corresponding to the most negative total energy, was retained.

The interaction energy is defined by:

$$\Delta E_{int} = E_{(complexe)} - (E_{additif} + E_{SARA}) \quad \text{(V.6)}$$

interaction energy, the stronger and more stabilising the interaction between the two species, reflecting a greater molecular affinity of the additive for the bituminous fraction under consideration. The results obtained for the 16 complexes are summarised in Table V.II.4 and illustrated graphically in Figure V.II.5.

Table V.II.4: Interaction energies ΔEint (kcal/mol) of the 16 additive-SARA complexes Calculated by Material Studio

Additive	SQUA (Saturated)	CORO (Aromatics)	ACID (Resins)	PORP (Asphaltenes)
PHEN (A_1)	-8.10	-11.54	-6.61	-13.80
BENZ (A_2)	-10.28	-15.18	-7.60	-15.08
PLAS (A_3)	-9.40	-12.93	-7.01	-14.31
WAX (A_4)	-15.49	-10.83	-5.26	-11.07

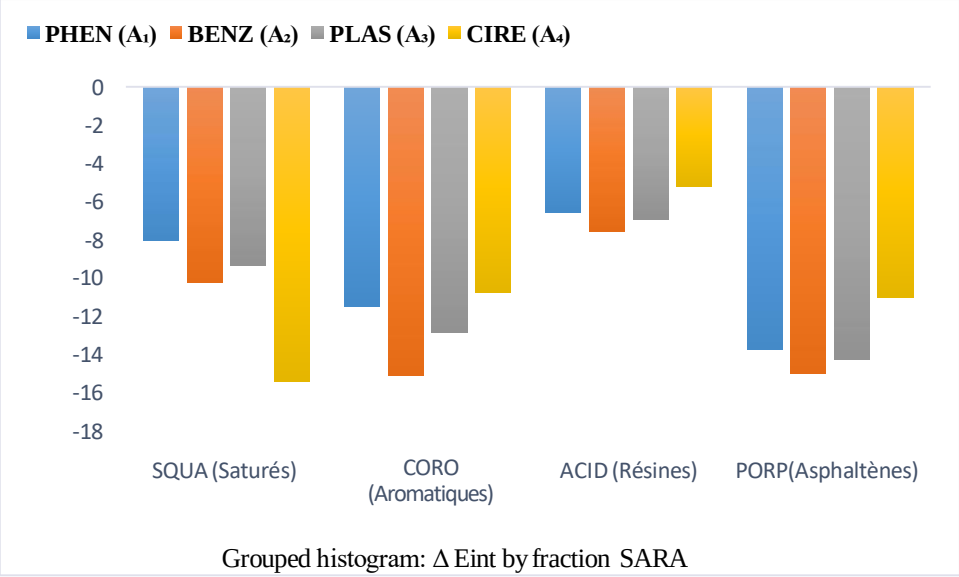


Figure V.II.5: Interaction energies ΔEint (kcal/mol) for 16 additive-SARA complexes.

Analysis of Table V.II.4 reveals that BENZ (A_2) exhibits the most negative interaction energies with CORO (−15.18 kcal/mol) and PORP (−15.08 kcal/mol), confirming its preferential affinity for aromatic and asphaltene fractions. PHEN (A_1) interacts preferentially with PORP (−13.80 kcal/mol) via O–H···N hydrogen bonding.

PLAS (A_3) shows a homogeneous interaction profile with all fractions, consistent with its role as a plasticiser. CIRE (A_4) stands out with its maximal interaction with SQUA (−15.49 kcal/mol), validating its insertion mechanism in saturated paraffins.

Table V.II.5: Interaction energies ΔEint (kcal/mol) of additives with the complete SARA system and molecular interpretation.

Additive	PHEN (A_1)	BENZ (A_2)	PLAS (A_3)	WAX (A_4)
ΔEint (kcal/mol)	-58.45	-66.94	-53.06	-52.74

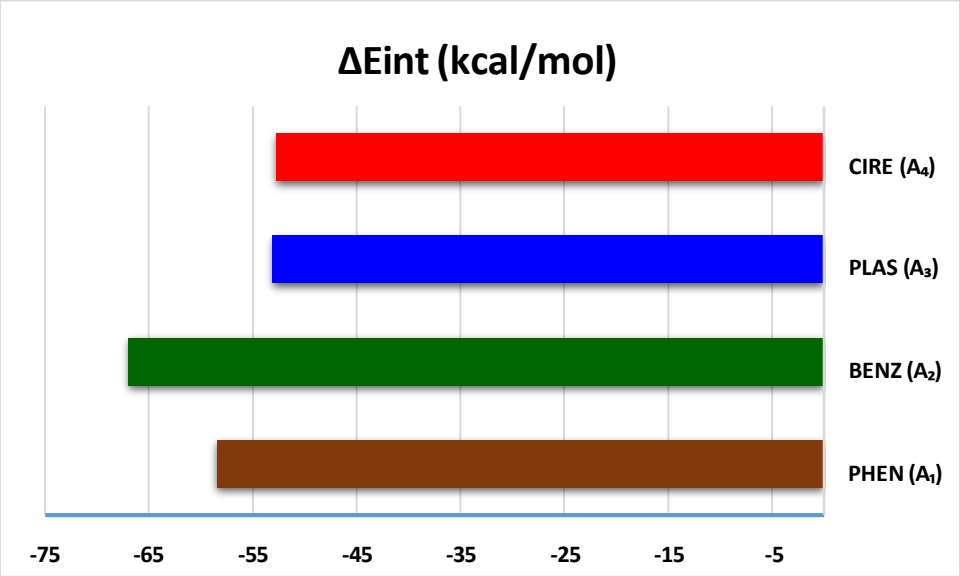


Figure V.II.6: Interaction energies ΔEint (kcal/mol) of the four additives with the complete SARA system (SQUA + CORO + ACID + PORP).

To simulate a more representative condition of the actual bituminous matrix, the interaction energies of the four additives were also calculated against the complete SARA system (SQUA + CORO + ACID + PORP combined).

The results in Table V.II.5 and Figure V.II.6 confirm the previously established ranking: BENZ (A_2) exhibits the most negative overall interaction energy (−66.94 kcal/mol), followed by PHEN (A_1) (−58.45 kcal/mol), PLAS (A_3) (−53.06 kcal/mol), and CIRE (A_4) (−52.74 kcal/mol).

The consistency between the two approaches (separate fractions and the complete system) strengthens the validity of the results obtained

Table V.II.6: non-covalent interactions of additive-SARA complexes analysed using Discovery Studio. Types, number and distances of π-π stacking interactions, and corresponding global interaction energies.

Additive	Type of interaction	Number	d min (Å)	d max (Å)	d moy (Å)	ΔEint (kcal/mol)
BENZ (A_2)	π–π Stacking	12	3.631	5.447	4.559	-66.94
PHEN (A_1)	π–π Stacking	1	3.680	—	—	-58.45
PLAS (A_3)	π–π Stacking	5	3.557	5,386	4,450	-53.06
WAX (A_4)	—	—	-----	-----	------	-52.74

Analysis of non-covalent interactions using Discovery Studio (Figure V.II.7) allows us to identify the nature of the interactions responsible for stabilising each additive-SARA complex. PHEN (A_1) exhibits a targeted π–π interaction at 3.680 Å with the aromatic fractions, indicating selective molecular insertion within the SARA matrix. BENZ (A_2) shows π–π interactions with coronene and an N–H···N hydrogen bond with Ni-porphyrin; despite an apparently limited number of interactions, their superior quality results in the most negative overall interaction energy (ΔEint = −66.94 kcal/mol). PLAS (A_3) exhibits π–π interactions with coronene and an O···Ni electrostatic interaction with the nickel atom of porphyrin. CIRE (A_4) is distinguished by van der Waals interactions between its long alkyl chain and the paraffinic fractions, confirming its mechanism physical action by insertion into the saturated chains of bitumen.

Comparison of the number of π–π interactions (Table V.II.6) and interaction energies (Tables V.II.4 and V.II.5) reveals a direct correlation: BENZ (12 interactions, ΔEint = −66.94 kcal/mol) > PLAS (5, −53.06) > PHEN (1, −58.45) > CIRE (0, −52.74). This correlation validates the consistency between the qualitative analysis of non-covalent interactions and the quantitative energy calculations, and confirms BENZ (A_2) as the most effective additive for stabilising the aromatic and asphaltene fractions of bitumen

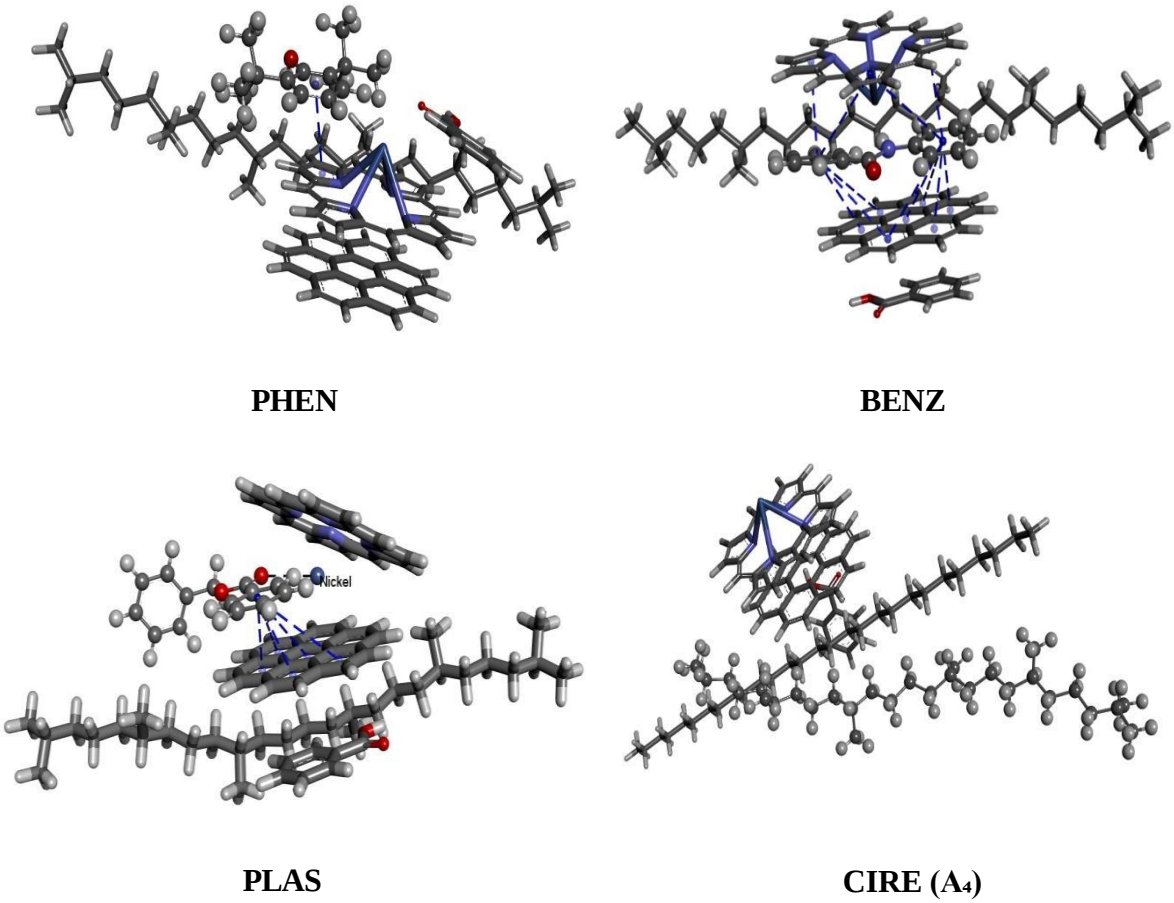


Figure V.II.7: Representation of non-covalent interactions of additives-SARA complexes (PHEN/A1, BENZ/A2, PLAS-A3, CIRE-A4) visualized under discovery

Conclusion

Conclusion

This work focused on the development and evaluation of stabilising additives designed to improve the storage stability and performance of 70/100 grade bitumen produced by the R1K refinery in Skikda.Given the susceptibility of this binder to oxidative ageing, colloidal instability, and increased viscosity during prolonged exposure to high storage temperatures, the aim was to identify, synthesise, and evaluate targeted chemical additives that could be formulated from precursors available in the Algerian industrial context.

Experimentally, three additives were successfully synthesised in the laboratory. 2,6-Di-tert-butylphenol (PHEN) was obtained by Friedel-Crafts alkylation of phenol with tert-butanol in sulfuric acid with a yield of 65–75%. N-Phenylbenzamide (BENZ) was prepared by acylation of aniline with benzoyl chloride in the presence of triethylamine in dichloromethane, with a yield of 85%. Benzyl benzoate (PLAS) was obtained by Fischer esterification in toluene with a yield of 90%. The agreement of the measured melting points with literature values and the consistency of the recorded UV-visible spectra with the expected chromophores for each structure provide a set of concordant data supporting the identity of the products obtained.

From a molecular modelling perspective, DFT calculations at the ωB97X-D/6-311++G(d,p) level provided a precise electronic description of the four additives. Analysis of the optimised geometries reveals conformations directly related to the function of each additive: PHEN adopts a planar conformation maximising the conjugation of the oxygen lone pair with the aromatic π system, thus enhancing its electron-donating character and antioxidant activity:

BENZ exhibits a quasi-planar geometry with a dihedral angle of 43.22°, favourable to π–π interactions with the polyaromatic sheets of asphaltenes: PLAS is planar around the C(=O)–O bond, characteristic of conjugated aromatic esters: CIRE adopts the all-trans conformation expected for n-octacosane.

The overall reactivity descriptors confirm the role assigned to each additive: BENZ exhibits the lowest HOMO-LUMO band gap (8.63 eV), indicating increased reactivity and a strong capacity for interaction with the polar fractions of asphaltenes: PHEN, with moderate electrophilicity (ω = 0.793 eV), validates its electron-donating character; CIRE, with the highest band gap (14.21 eV) and maximum hardness (η = 7.10 eV), confirms its chemically inert character, acting exclusively through van der Waals interactions.

The analysis of the interaction energies of the sixteen additive-SARA binary complexes, calculated using the COMPASS III force field in Material Studio and visualised by Discovery Studio, demonstrates the remarkable complementarity of the four additives with respect to the

constituent fractions of bitumen. BENZ exhibits the most negative total interaction energy with the complete SARA system (ΔEint = −66.94 kcal/mol), driven by twelve π–π stacking interactions, confirming its superior ability to stabilise asphaltene and coronene aggregates.

PHEN interacts preferentially with Ni (II) porphyrin, the model for asphaltenes, with an energy of −13.80 kcal/mol via O–H···N bonds directly involved in radical inhibition. PLAS shows a homogeneous interaction profile with all fractions (total ΔEint = −53.06 kcal/mol), consistent with its role as a non-specific plasticiser. CIRE stands out due to its maximum affinity for the saturated squalane fraction (ΔEint = −15.49 kcal/mol), validating its physical mechanism of insertion into the paraffin chains of Algerian bitumen. The consistency between the qualitative analysis of non-covalent interactions and the energy quantification strengthens the credibility of all the conclusions drawn.

In summary, the synergistic combination of the three synthesised additives covers all the degradation mechanisms of 70/100 bitumen from the R1K refinery: PHEN counteracts radical oxidation, BENZ delays the sedimentation of asphaltenes, and PLAS lowers the application viscosity.

The expected temperature reduction, on the order of 20 to 40 °C, is compatible with the requirements of warm mix asphalt technologies, the large-scale deployment of which in the Algerian context would represent a considerable economic and environmental gain for NAFTAL and the entire national road construction sector. This study thus contributes to the establishment of a molecular theoretical framework for the rational design of new multifunctional additives adapted to Algerian bitumen.

Several perspectives naturally emerge from this work. In the short term, acquiring FTIR and ^{1}H and ^{13}C NMR spectra of the synthesised additives will allow us to complete their structural confirmation, currently based on melting points and UV-visible spectra. In the medium term, incorporating these additives into actual 70/100 bitumen formulations from the R1K refinery, followed by a complete rheological evaluation using the standardised RTFOT, PAV, DSR, and BBR protocols,will allow us to experimentally validate the predictions derived from molecular modelling. In the longer term, extending DFT calculations to ternary complexes with explicit BSSE correction and implementing molecular dynamics simulations will allow us to study the temporal evolution of asphaltene aggregates in the presence of the additives at different storage temperatures.

A collaboration with the laboratories of the R1K refinery in Skikda and with SONATRACH for validation under real industrial conditions would constitute the natural and necessary outcome of this research program.

الجمهورية الجزائرية الديمقراطية الشعبية
Popular and democratic of Algeria
وزارة التعليم العالي و البحث العلمي
Minister of higher education and scientific research

University Of 20 August 1955 Skikda		جامعة 20 أوت 1955 - سكيكدة
Faculty of science	SKIKDA	كلية العلوم
department of chemistry		قسم الكيمياء

Le : 16/07/2026

Autorisation de dépôt de Mémoire de Master

Je soussigne : Dr. Chettat Faiza

Certifier que l'étudiant (e) :

Gabli Aya

Spécialité : Chimie organique

Intitulé :
Synthesis and Molecular Modelling of Stabilising Additives for Bitumen Storage at Reduced Temperature

A apporté les corrections relatives à son travail de mémoire de Master.

Visa de L'encadrant

Scanné avec CamScanner